A SIMULATION STUDY OF COOPERATIVE UNDERWATER ACOUSTIC COMMUNICATION

A Thesis

by

Hamza Ümit Sökün

Submitted to the
Graduate School of Sciences and Engineering
In Partial Fulfillment of the Requirements for
the Degree of

Master of Science

in the
Department of Electrical and Electronics Engineering

Özyeğin University
August 2012

A SIMULATION STUDY OF COOPERATIVE UNDERWATER ACOUSTIC COMMUNICATION

Approved by:

Professor Murat Uysal, Advisor
Department of Electrical and Electronics Engineering
Özyeğin University

Professor Habib Şenol
Department of Electrical and Electronics Engineering
Kadir Has University

Professor Tanju Erdem
Department of Electrical and Electronics Engineering
Özyeğin University

Date Approved: 1 August 2012

To my parents

ABSTRACT

Cooperative communication promises significant performance gains in terms of link reliability, spectral efficiency, system capacity, and transmission range. Due to its indisputable advantages for high-speed underwater applications with size and power limitations, cooperative transmission is a promising physical layer solution for next generation underwater acoustic (UWA) communication systems. Although a rich literature already exists on cooperative communication for terrestrial wireless radio frequency (RF) systems, there are only sporadic results reported for UWA applications. In this thesis, we consider cooperative UWA communication and investigate the performance of relay selection in underwater for multi-carrier and single-carrier systems with various selection criteria.

In the first part, we consider a multi-carrier multi-relay cooperative UWA communication system based on orthogonal frequency division multiplexing (OFDM) and investigate both amplify-and-forward (AaF) and decode-and-forward (DaF) relaying in half-duplex mode. We adopt different relay selection criteria which rely either on the maximization of signal-to-noise ratio (SNR), the minimization of probability of error (PoE), or the maximization of capacity for relay selection. These are utilized in conjunction with diverse approaches such as per-subcarrier, all-subcarriers, or subcarrier grouping. We provide an extensive Monte Carlo simulation study to evaluate the error rate performance of relay selection schemes.

In the second part of the research, in order to increase spectral efficiency, we consider OFDM-based multi-relay systems with two-way relaying and study the performance of relay selection in UWA channels.

In the final part of the thesis, we consider single-carrier frequency-domain equalization (SC-FDE) and present the performance of relay assisted SC-FDE schemes providing comparisons with uncoded OFDM counterparts.

ÖZETÇE

İşbirlikli haberleşme, bağlantı güvenirliliği, spektral verimlilik, sistem kapasitesi ve iletim menzili açısından önemli kazanımlar vaat eder. Özelikle fiziksel boyut ve güç kısıtlamalı yüksek hızlı sualtı uygulamaları için tartışılmaz avantajlarından dolayı, işbirlikli haberleşme, gelecek nesil sualtı akustik haberleşme sistemleri için potansiyel vaat eden bir fiziksel katman çözümüdür. Karasal kablosuz radyo frekans sistemlerinde, işbirlikli haberleşme üzerine halihazırda zengin bir literatür olmasına karşın sualtı akustik uygulamaları için sadece tek tük sonuçlar vardır. Bu tezde, işbirlikli sualtı akustik haberleşmesi ele alınmış ve çeşitli seçim kriterleri ile çok taşıyıcılı ve tek taşıyıcılı sistemler için sualtı röle seçim başarımı incelenmiştir.

Tezin ilk kısmında, dik frekans bölmeli çoğullama tabanlı çok taşıyıcılı ve çok röleli işbirlikli sualtı akustik haberleşme sistemleri ele alınmış ve yarı çift yönlü modda çalışan yükselt-ve-ilet ve çöz-ve-ilet röleleme teknikleri incelenmiştir. Röle seçimi için sinyal-gürültü oranını enbüyütme, hata olasılığını enküçütme veya kanal sığasını enbüyütmeye dayanan farklı seçim kriterleri kullanılmıştır. Bunlar alttaşıyıcı başına, tüm altaşıyıcılar ve alttaşıyıcı gruplandırılması gibi farklı yaklaşımlarla beraber ele alınmıştır. Röle şeçim yapılarının hata başarımı, kapsamlı bir Monte Carlo benzetim çalışması aracılığıyla ortaya konulmuştur.

Araştırmanın ikinci bölümündeyse, spektral verimliliği artırmak için, çift yönlü röleleme tekniğinin kullanıldığı dik frekans bölmeli çoğullama tabanlı ve çok röleli işbirlikli sualtı akustik haberleşme sistemi ele alınmış ve sualtı akustik kanallardaki röle şeçim başarımı incelenmiştir.

Tezin son kısmında ise tek taşıyıcılı frekans bölgesi denkleştirme sistemi ele alınmış ve sualtı akustik kanallarındaki hata başarımı, kodlamasız dik frekans bölmeli çoğullama

sistemininkiyle kıyaslanarak ortaya konulmuştur.

ACKNOWLEDGEMENTS

First and foremost, I would like to express my deepest appreciation and sincere gratitude to my advisor Prof. Murat Uysal for giving me the opportunity to work with him in the Communication Theory and Technologies (CT&T) Research Group at Özyeğin University. His valuable support, suggestions and comments made this work possible. None of these would have been possible without his help.

The National Scholarship Programme for M.Sc. awarded by Turkish Scientific and Research Council (TÜBİTAK) was crucial to start my graduate studies and made this journey possible.

It is my pleasure to thank my thesis committee members, Dr. Tanju Erdem and Dr. Habib Şenol for their valuable time and efforts.

Words cannot express my heartiest thanks and gratitude to my parents for their unconditional love, support and encouragement throughout this work.

Finally, special thanks to Dr. Bahattin Karakaya for his insightful discussions and cooperation.

TABLE OF CONTENTS

LIST OF TABLES

LIST OF FIGURES

CHAPTER I

INTRODUCTION

1.1 Background

Underwater wireless communication has received much attention over the last few years. This has been triggered by the increasing demand for reliable high-speed wireless links to accommodate a wide range of underwater applications, including offshore oil field exploration/monitoring, oceanographic data collection, maritime archaeology, environmental monitoring, disaster prevention, and port security among many others [3]. Although wire-line systems have been used to provide real-time communication in some underwater applications, their high cost and operational disadvantages become restrictive for many cases. Wireless communication is a promising alternative and an ideal transmission solution for underwater applications.

The wireless transmission of information underwater can be achieved through radio, optical, or sound waves [4]. Although radio and optical waves can be used for very short range applications, acoustic signals are preferred for communicating underwater. Due to the high attenuation of seawater, long-range RF communication is problematic and requires the use of extra low frequencies which require large antennas and high transmit powers. Although early military deployment of underwater RF communications is known, the first commercial underwater RF modem was introduced only back in 2006 [5]. Optical waves do not suffer from the attenuation as much, but are severely affected by absorption, scattering, and high level of ambient light limiting the transmission ranges. Thus, among the three types of waves, acoustic transmission is the most practical and commonly employed method due to favorable propagation characteristics of sound waves in the underwater environments. A comparison of these

three transmission techniques is given in Table 1 [5].

Table 1: Comparison of acoustic, radio and optical waves.

	Acoustic	Radio	Optical
Speed of Sound (ms^{-1})	1.500	3.10^{-8}	3.10^{-8}
Bandwidth	$\sim$ kHz	$\sim$ MHz	$\sim$ 10-150 MHz
Antenna Size	$\sim$ 0.1 m	$\sim$ 0.5 m	$\sim$ 0.1 m
Frequency Band	$\sim$ kHz	$\sim$ MHz	$\sim 10^{14} - 10^{15}$ MHz
Effective Range	$\sim$ km	$\sim$ 10 m	$\sim$ 10-100 m
Attenuation	low	high	high
Data Rate	up to 100 kbps	up to 10 Mbps	up to 1 Gbps
Major hurdles	bandwidth-limited	power-limited	environment-limited

1.2 UWA Communications

1.2.1 Early Research Efforts

Some sea animals such as dolphins and whales have been using underwater acoustics for communication and object detection for millions of year. However, humankind has not comprehended this transmission medium until late 14th century when renowned painter, polymath Leonardo Da Vinci is quoted for discovering the possibility of using sound to detect distant ships by listening to the noise they radiate into water [6]. During the 1800s, the first experiments to investigate the speed of sound in water were conducted by various scientists. In 1877, the British scientist John William Strut formulated the wave equation and mathematically described sound waves which form the basis for acoustics.

During World War I, the need to detect submarines sparked more research efforts on the use of underwater acoustics. The development of UWA communication was however later in the era of World War II during which US navy developed first underwater telephones for communication with submarines. The first UWA telephones operated at 8 - 11 kHz and these analog devices employed single-side band suppressed

carrier (SSB - SC) modulation as the modulation type. Until 1980's, the research efforts on UWA communication were mainly dominated by military applications. Following the advances of DSP and VLSI technologies, new generations of digital UWA communication systems were introduced targeting a variety of applications for the civilian market [7].

1.2.2 Digital UWA Communications

Most of the early digital UWA communication systems used non-coherent modulation schemes. It was commonly believed then that the time variability and the dispersive multipath propagation characteristics of the ocean would not allow the use of phase-coherent modulation techniques such as phase shift keying (PSK) and quadrature amplitude modulation (QAM). For these initial systems, the prevailing choice was frequency-shift keying (FSK) modulation, [8] despite its very low data rates and bandwidth inefficiency.

In 1990's, with the increasing demands for higher data rates, research focus shifted towards the design of coherent acoustic modems. One approach towards this purpose, such as in [9, 10, 11], was to employ differentially-coherent detection to ease the problematic carrier recovery in underwater channel. However, differential techniques inevitably result in performance degradation with respect to coherent detection. In [12], Stojanovic et. al. adopted "purely" phase-coherent detection and designed a receiver built upon adaptive joint carrier synchronization and equalization. The optimum maximum likelihood (ML) algorithm for such a joint estimator suffers from excessive complexity particularly for the underwater channel characterized by long channel impulses. Therefore, as a low-complexity solution, the receiver algorithm in [12] adopts decision feedback equalizer (DFE) whose taps are adaptively adjusted using a combination of RLS (recursive least squares) algorithm and second-order PLL (phase locked loop).

1.2.3 Current Research Efforts and Future Ahead

Since the seminal work of Stojanovic et. al. in [12], there has been a growing interest on coherent UWA communication systems. Much research effort has particularly focused on the design of low-complexity equalization schemes, which is a key issue for underwater channels with large delay spreads. Particularly, sparse channel estimation/equalization [13, 14, 15, 16, 17, 18] and turbo equalization [19, 20, 21, 22, 23, 24] have been investigated by several researchers.

As an attractive alternative to time-domain equalization, OFDM has been also applied to UWA communication, see e.g., [25, 26, 27, 28, 29, 30]. In an OFDM system, channel distortion can be compensated at the receiver on a subcarrier-by-subcarrier basis eliminating the need for complex time-domain equalizers which is a limiting design factor for UWA communication systems.

Emerging data-heavy underwater applications impose further requirements on UWA communication system design. To address such challenges, recent advances in terrestrial wireless RF systems have been further exploited in the context of UWA communication. One of the research breakthroughs in the last decade is multiple-input multiple-output (MIMO) communications. MIMO systems involve the deployment of multiple antennas at the transmitter and/or receiver side and achieve significant improvements in transmission reliability and throughput. For example, in [31], Roy et. al. investigated the application of space-time trellis codes and layered space-time codes in UWA communication systems. Through simulations and real-life experiments, they demonstrated significant improvements over conventional single-input single-output (SISO) systems in terms of data rates and reliability.

Although MIMO systems successfully exploit the spatial dimension, their practical implementation over frequency-selective channels (as encountered in underwater channels) is challenging considering the potential high complexity of spatio-temporal equalizers. This has further sparked interest into research on the combination of

MIMO and OFDM for underwater channels, see e.g. [32, 33, 34] and the references therein.

Another promising approach in the design of future UWA communication systems is the potential deployment of cooperative communication techniques (see Figure 1) which will be the focus of this thesis. In the following, we first provide an overview of cooperative communication (also known as "user cooperation" or "cooperative diversity") [35] and then describe the state-of-the art in cooperative UWA communications.

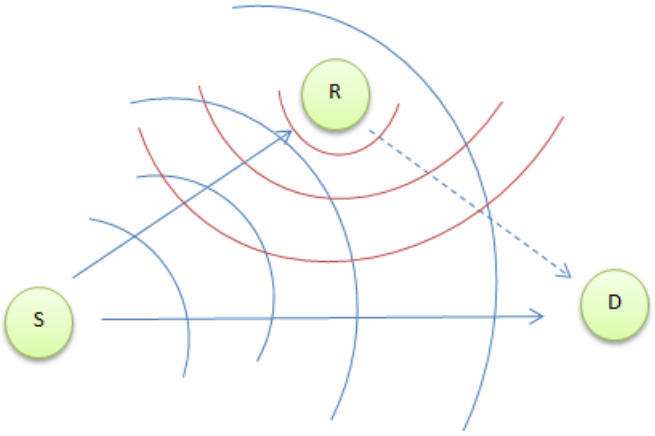

Figure 1: Illustration of cooperative communication.

1.3 Cooperative Diversity

Cooperative diversity exploits the broadcast nature of wireless transmission and relies on the cooperation of users relaying each other's information. When a source node transmits its signal, this is received by the destination node and also overheard by other nodes in the vicinity. If these nodes are willing to share their resources, they can forward the overheard information to the destination as a second replica of the original signal and act as relays for the source node extracting a diversity order on the number of relays.

In 1970's, Van der Meulen [36] introduced the concept of relay channel and Cover and Gamal [37] demonstrated the information theoretical analysis of additive white

Gaussian noise (AWGN) relay channels. The recent surge of interest in cooperative communication, however, was subsequent to the publications of Sendonaris et. al.'s and Laneman et. al.'s in 2003-2004. Laneman et.al. [38, 39] extended the concept of relaying to more general cooperative communication taking into account the effect of fading. They demonstrated that full spatial diversity can be achieved through user cooperation.

In [40], Nabar et al. established a unified framework of time division multiple access (TDMA)-based cooperation protocols for single-relay wireless networks. They quantified achievable performance gains for distributed schemes in an analogy to conventional co-located multi-antenna configurations. Specifically, they considered three protocols named "Protocol I", "Protocol II" and "Protocol III". In an independent work by Ochiai [41], they are referred as "Transmit Diversity (TD) Protocol", "Receive Diversity (RD) Protocol" and "Simplified Transmit Diversity (STD) Protocol". In TD protocol, the source terminal communicates with the relay and destination during the first phase (i.e., broadcasting phase). During the second phase (i.e., relaying phase), both the relay and source terminals communicate with the destination terminal. In RD protocol, the source terminal communicates with the relay and destination terminals in the first phase. This protocol is the same as "orthogonal relaying" proposed originally in [38]. In the second phase, only the relay terminal communicates with the destination. STD protocol is essentially similar to TD protocol except that the destination terminal does not receive from the source during the first phase [42].

Cooperative schemes can work either with DaF or AaF relaying. These are also known as regenerative relaying and non-regenerative relaying, respectively (see Figures 2 and 3). In DaF relaying, the relay node fully decodes, re-encodes, possibly using a different codebook, and retransmits the source node's message. The DaF

protocol has the well-known disadvantage of error propagation. The relays can forward erroneous information, and these errors propagate to the destination [43]. To avoid this, practical implementation requires the use of error detection methods such as cyclic redundancy check (CRC) at the relay terminal.

In AaF relaying, the relay retransmits a scaled version of the received signal without any attempt to decode it. There are two different type scaling factors due to availability of the channel state information (CSI) at the relay terminal. In CSI-assisted AaF scheme, the relay makes use of instantaneous CSI of the source-to-relay link to scale its received noisy signal. On the contrary, blind AaF scheme does not use to CSI and employs fixed power constraint [42]. The scaling factors for CSI-assisted and blind AaF schemes are referred as average power scaling (APS) and instantaneous power scaling (IPS) constraints in [44], respectively.

Most cooperative systems operate in half-duplex mode, known as one-way transmission, and devote two time slots for each single packet transmission. This systems leads spectral inefficiency. A method to improve spectral efficiency is two-way (bi-directional) relaying [45, 46, 47, 48, 49]. In two-way relaying, two terminals exchange their information through a single or multiple common relays. In the first phase, two sources transmit messages to relays in the same frequency band and same time slot. In the second phase, the relay broadcasts its normalized signal to both sources in the same frequency band and the same time slot. Each source therefore receives the information of its counterpart. Based on the fact that each source has knowledge of its own originally transmitted data, both sources cancel their self-interference from the received signal to recover the data of other terminal. Thus, two-way communication requires only two time slots, while one-way communication needs four time slots to exchange the same information in half-duplex transmission.

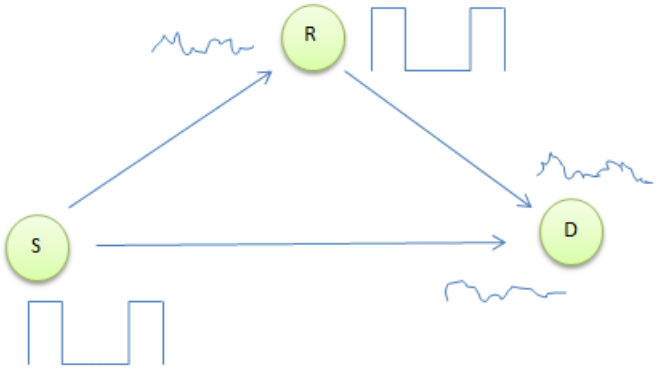

Figure 2: Illustration of decode-and-forward relaying.

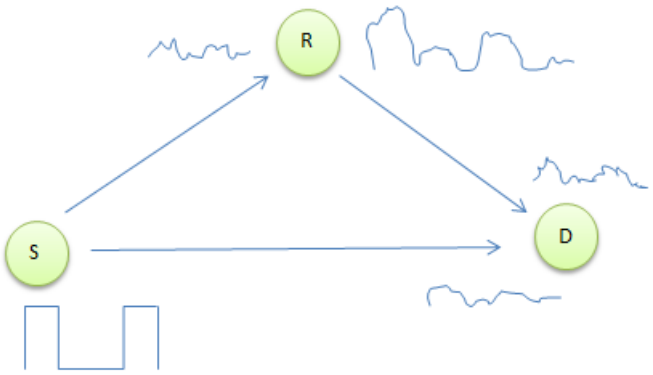

Figure 3: Illustration of amplify-and-forward relaying.

1.3.1 Cooperative UWA Communication

There has been a growing literature on how the principles of cooperative communication can be applied to UWA systems, see e.g. [50, 51, 52, 53, 54, 55]. In [50], the capacity of a relay channel is shown to increase with the number of relays. Since relaying also helps to reduce the total transmission power, its benefits on an acoustic link are even more pronounced in view of the energy per bit savings. In [51], multi-hop cooperation schemes for underwater sensor networks are studied and shown to be highly energy efficient. In [52], cooperation protocols coupled with space-time block coding (STBC) are proposed and analyzed for distributed cooperation communication. In [53], simulation results are provided to show that the quality of image transmissions is improved by relay-assisted transmission. In [54], information theoretical performance of several cooperative transmission schemes are studied in an underwater scenario, and a new wave cooperation transmission scheme is designed by taking advantage of the low propagation speed of sound for the underwater environment. In [55], cooperative transmission has been studied from an energy consumption point of view in underwater taking into account the effects of time-varying channel.

1.4 Contributions of the Thesis

The advantages of cooperative diversity come at the expense of a loss in spectral efficiency since the source and all the relays must transmit in orthogonal channels. The inefficient utilization of the channel resources can be mitigated by relay selection (see Figure 4) without sacrificing the diversity advantages of cooperative transmission. In such an approach, a set of relays, or only one relay is selected based on the predetermined relay selection criteria to cooperate with the source to transmit the messages to the destination. Additionally, relay selection achieves higher throughput since fewer time slots are required to complete transmission of one block. It also eases synchronization requirements in cooperative systems.

In the literature, there already exists a rich literature on relay selection in the context of terrestrial RF communication systems (see [56, 57, 58, 59, 60, 61] and the references therein). However, the number of publications on relay selection in UWA communication systems is sporadic [62, 63]. In [62], an efficient cooperative automatic repeat request (ARQ) scheme was proposed for multi-hop UWA communications in order to improve throughput efficiency. In this scheme, when the relay node receives an erroneous packet, it asks for retransmission from a cooperative node, which is selected in a closest-one-first manner from the nodes in the cooperative region. The selection procedure continues until the retransmission is successful. In [63], the application of cooperative communication protocols to multi-carrier underwater networks was investigated assuming DaF and AaF relaying techniques. Particularly, it studied the performance of SNR maximization based relay selection method in conjunction with all-subcarriers approach by taking into account of existence of small-scale fading.

In this thesis, we consider an aggregate channel which combines the effect of large-scale transmission loss and small-scale fading. As detailed in Chapter II, we employ an underwater propagation software named Bellhop [64] for a realistic channel characterization. We consider an OFDM-based multi-carrier multi-relay cooperative UWA communication system and investigate both AaF and DaF relaying in half-duplex mode. We adopt relay selection criteria which rely either on the maximization of SNR, the minimization of PoE, or the maximization of capacity for relay selection. These are utilized in conjunction with different approaches such as per-subcarrier, all-subcarriers, or subcarrier grouping. We provide an extensive Monte Carlo simulation study to evaluate the error rate performance of different relay selection schemes.

In the second part of the research, in order to improve spectral efficiency, we consider OFDM systems with two-way relaying and study the performance of relay selection in UWA channels.

In the final part of research, we consider SC-FDE as an alternative to OFDM.

SC-FDE provides a similar performance to OFDM with almost same overall complexity. This single-carrier technique was only very recently applied to underwater communications for point-to-point links [65, 66, 67], however no research results have been yet reported for cooperative scenarios. In this part, we present the performance of relay assisted SC-FDE schemes assuming linear equalization techniques such as zero forcer (ZF) and minimum mean square error (MMSE).

The rest of this thesis is organized as follows: In Chapter II, we consider a multi-carrier and multi-relay network operating in AaF mode for UWA communication, where RD cooperation protocol is employed and investigate the error rate performance of relay selection. In Chapter III, we extend our investigation for DaF relaying. In Chapter IV, we evaluate the performance of a multi-carrier and multi-relay network operating in AaF mode with two-way relaying rather than conventional one-way communication. In Chapter V, we present performance results of a single-relay cooperative SC-FDE system for UWA communication as an alternative to OFDM. Finally, in Chapter VI, we conclude the thesis.

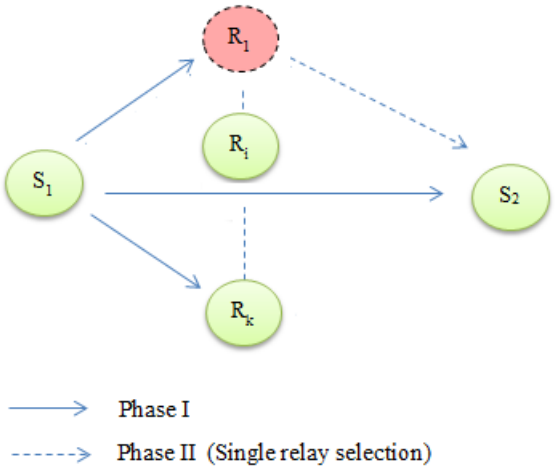

Figure 4: Illustration of relay selection.

CHAPTER II

UWA CHANNEL MODEL

2.1 Introduction

The characteristics of UWA channel are strikingly different from well known RF channel models. The channel exhibits frequency-dependent transmission loss, time-varying multipath, non-white Gaussian ambient noise and extreme Doppler effect. High and variable propagation delay due to low speed of sound, (i.e. 1500 m/s) is a fundamental feature of UWA channel. Thus, it can be considered as a combination of the worst properties of RF channels, i.e. poor physical link quality of a mobile terrestrial radio channel, and the high latency of a satellite channel [2].

2.2 Basic Characteristics of UWA Channel Model

In this section, we summarize some fundamental characteristics of UWA channel.

2.2.1 Propagation Delay

The speed of sound in water is approximately four times faster than the speed of sound in air, and is five orders lower than that of light. It depends on temperature, salinity, and pressure (related to depth). Let T be the temperature in degrees Celsius, S the salinity in parts per thousand and z the depth in meters. The speed of sound in water can be expressed by [68]

$$c = 1448.96 + 4.519T - 0.05304T^2 + 0.0002374T^3 + 1.340(S-35) + 0.0163z + 1.675 \times 10^{-7}z^2 - 0.01025T(S-35) - 7.139 \times 10^{-13}Tz^3 \quad (1)$$

where $0 \leq T \leq 30^o$, $30 \leq S \leq 40$ and $0 \leq z \leq 8000$.

In Figure 5, the velocity profile is divided into layers with different characteristics. Just below the sea surface is the surface layer where the sound velocity varies with the local variations such as heating, cooling, and wind action. Below the surface layer lies the seasonal thermocline where temperature decreases with depth according to seasons. Below the seasonal thermocline is the main thermocline where the temperature decreases fastly with increasing depth. Below the main thermocline and extending to the sea bottom is the deep isothermal layer, where the temperature is nearly constant and in which the sound speed increase with the depth due to the effect of pressure on sound velocity. This velocity profile changes with latitude, season, time of day, and meteorological conditions [69].

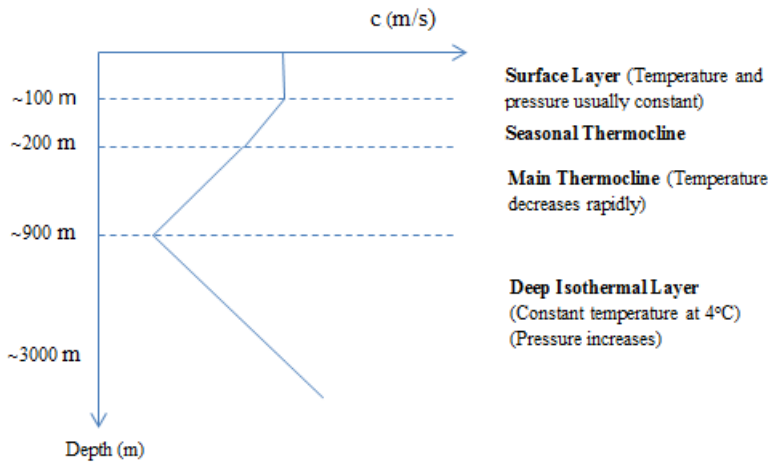

Figure 5: Speed of sound in underwater.

2.2.2 Transmission Loss

Transmission loss primarily depends on attenuation and spreading loss. Attenuation includes the effect of absorption and scattering, and varies linearly with range. Absorption loss occurs when acoustic energy is converted into heat. The ocean sound is attenuated by two main mechanisms named viscous absorption (viscosity can be described as the resistance of a fluid to flow) and ionic relaxation effects due to the

presence of tiny concentrations of boric acid and magnesium sulfate salts in sea water. The effect of viscous absorption is significant at high frequency (above 100 kHz), whereas the ionic relaxation effects due to boric acid affect at low frequency (up to a few kHz), and due to magnesium sulfate affect at intermediate frequencies (up to a few 100 kHz) [70].

Several empirical formulas have been developed over the years for the characterization of the absorption coefficient including Schulkin-Marsh (1962) [71], Thorp (1965) [72], Mellen-Browning (1976) [73], Fisher-Simmons (1977) [74], and Francois-Garrison (1982) [75, 76]. At the low frequencies 100 Hz - 3 kHz, the absorption coefficient can be calculated by Thorp's formula [72]:

$$\alpha(f) = \frac{0.1f^2}{1+f^2} + \frac{40f^2}{4100+f^2} + 2.75 \times 10^{-4} f^2 + 0.003. \tag{2}$$

The more extensive form of Thorp's formula is Francois-Garrison's (FG) formula, and it is valid between 100 Hz - 1 MHz.

Sound can be scattered by particles and objects along the propagation path, resulting in energy loss. The amount and locations of scatterers in water can vary from time to time in a given area. Besides random scattering, sound wave is refracted at the boundary of different water conditions [54]. It is not possible to distinguish between absorption and scattering effects in real-life experiments. Both phenomena contribute to the sound attenuation in sea water.

Spreading loss is a geometrical effect representing the regular weakening of a sound signal as it spreads outward from the source. There are two kinds of spreading factor. First one is spherical spreading factor which is caused by radiation of the power generated from a point source in all directions on the surface of a sphere. The second one is cylindrical spreading factor which exists when the medium is constrained by two reflecting planes. Its values are between 1 and 2 for cylindrical and spherical spreading, respectively. Depending on the spacial boundary of the water, the spreading loss can be modeled as either spherical for deep water or cylindrical for shallow water. A

spreading factor of 1.5 is often taken as representative of practical spreading based on a partially bounded sphere.

Therefore, overall transmission loss is given by [70]:

$$TL = k \times 10\log_{10} r + \alpha(f) r \times 10^{-3} \tag{3}$$

where $\alpha(f)$ represents the absorption coefficient (dB/km), r is the range expressed in meters and k is spreading loss factor.

In our channel model, we will use the Bellhop software which uses the principles of ray tracing for the calculation of the transmission loss. This software precisely reflects the characteristics of a geographical location such as sound speed profile (SSP), sound frequency, bathymetry, the type of bottom sediments, depths of nodes, etc. In Bellhop, transmission loss along each ray tube is given in decibels (dB) [77] with respect to a measurement point, i.e.,

$$TL(s) = -20 \log \frac{p(s)}{p_o} \tag{4}$$

where $p(s)$ is the pressure at a point a distance s from the source, and p_0 is the intensity measured at 1 m from the source.

2.2.3 Fading

Multipath propagation occurs whenever there is more than one propagation path between source and receiver. When a source launches a beam of rays, each ray will propagate over a different path and arrive at the receiver with diverse delays. The signal power is degraded as a result of overlapping of multiple echoes with each other. The time difference between the first and the last arrivals is called as delay spread which is relatively high as compared to the terrestrial radio channel because of low speed of sound in water. The length of delay spread may be on the order of tens of milliseconds, or more. This implies that the inter-symbol interference (ISI) in a single-carrier broadband system may span tens or even hundreds of symbol intervals;

a situation very different from that typically found in radio systems, where ISI may involve a few symbols only [78]. As the average received power is calculated by using transmission loss, the instantaneous level of the received power fluctuates due to small-scale fading which is caused by multipath propagation.

Multipath propagation primarily depends on depth, but it is also affected by frequency and transmission range. Based on the depth, occurrence of multipath is based on different reasons. In a shallow water environment, reflections of acoustic wave from surface and bottom, and direct path induce the multipath propagation. In a deep water, the spatial variation of sound speed causes bending of rays. This is because a ray of sound always bends toward the region of lower propagation speed, obeying Snell's law. Therefore, ray bending is the main phenomenon in deep water as well as surface and bottom reflections may be negligible. In Figure 6, the propagation of sound in both shallow and deep water are provided.

In a multipath environment, each path is assumed to act as a low pass filter, and thereby the impulse response is given by [2]

$$h(t) = \sum_{p} h_p(t - \tau_p), \tag{5}$$

where $h_p(t)$ is path gain and τ_p refers to the path delay of the pth path. The impulse response of UWA channel includes a large number of zero taps. This is because the UWA channel is sparse, and its energy is gathered around several small regions.

Numerous studies have been conducted to stochastically model the path gains. These studies are usually based on experimental acoustic data collected in a particular location. Different statistical models have been proposed depending on the location of the experiment, the type of signals used for probing, and the time intervals during which the channel is observed. Although there is not a general consensus, Ricean or Rayleigh fading is widely used for UWA channels [79].

The UWA channel is also subject to time-selectivity. Even in fixed underwater

applications, the channel exhibits Doppler spread due to surface scattering and internal waves. In mobile underwater applications, the Doppler spread is determined by the movement of the vehicle. Doppler distortion of an acoustic signal can be extreme because the speed of sound is very low. An effective method to solve the Doppler problem is through resampling operation as discussed in [80].

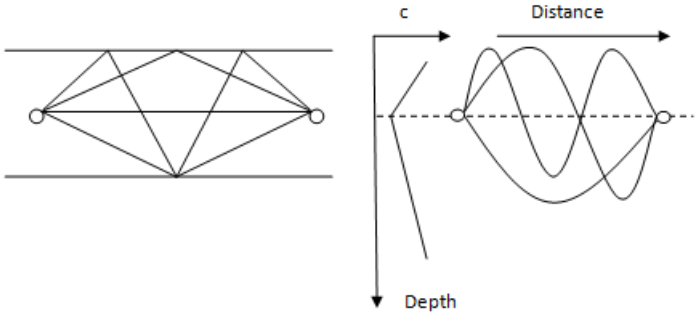

Figure 6: Multipath propagation in shallow and deep water [2].

2.2.4 Noise

Noise in an acoustic channel consists of ambient noise and site-specific noise. While ambient noise is always present in the background of quiet deep sea, site-specific noise exists only in certain places [2]. Site-specific noise could be caused by ice cracking in polar regions, snapping shrimp in warmer waters, seismic events and rain. Also, it exhibits non-Gaussian characteristics. On the contrary, ambient noise is induced by turbulence in the ocean and atmosphere, distant ship traffic, surface agitation caused by wind-driven waves, and thermal noise. This noise is often modeled as non-white Gaussian. According to the Wenz model [81], there are four main noise sources each of which becomes dominant in different frequency regions, namely turbulence (N_t),

shipping (N_s), wind (N_w), and thermal (N_{th}) :

$$10\log_{10}N_t(f) = 17 - 30\log_{10}(f) \tag{6}$$

$$10\log_{10}N_s(f) = 40 + 20(sa - 0.5) + 26\log_{10}(f) - 60\log_{10}(f + 0.03) \tag{7}$$

$$10\log_{10}N_w(f) = 50 + 7.5\sqrt{w} + 20\log_{10}(f) - 40\log_{10}(f + 0.4) \tag{8}$$

$$10\log_{10}N_{th}(f) = -15 + 20\log_{10}(f) \tag{9}$$

where sa is shipping factor, w is the speed of wind (m/s), and f is in kHz. The shipping activity lies between 0 (no activity) and 1 (maximum activity).

The total ambient noise is obtained as

$$N(f) = N_t(f) + N_{sa}(f) + N_w(f) + N_{th}(f) \tag{10}$$

In the frequency range below 10 Hz, turbulence in the ocean and atmosphere is the primary noise source. In the frequency range between 10 - 100 Hz, noise caused by distant ship traffic dominates and is modeled by shipping activity factor. Surface agitation caused by wind-driven waves becomes the major noise source in the frequency range of 100 Hz - 100 kHz that spans the major operating frequencies in UWA communication systems. The wind speed w is the main determining parameter for this type of noise. At frequencies above 100 kHz, thermal noise as a result of the molecular motion in the sea becomes the dominating factor.

2.3 Underwater Channel Modelling

2.3.1 Ray Tracing Methods

The propagation of sound in the water can be described by use of wave equations of the acoustic field in which parameters and constraints mathematically define the ocean environment. However, the associated computational complexity renders exact calculations infeasible for most practical purposes. For approximate numerical solutions, four diverse modeling techniques, namely Ray theory, Normal mode (NM), Fast Field Program (FFP) and Parabolic Equation (PE) are widely used.The choice

of model mainly depends on the desired tradeoff between accuracy, run time and ease of use.

Among these four techniques, ray theory models are particularly attractive with their computational efficiency. The ray tracing method consists of approximating a given source by a fan of beams and tracing the propagation of these beams through the medium [82]. Occurrence of shadow zones and caustics [83] are considered a main disadvantage of this model. However, one of ray tracing variants, i.e., Gaussian beam tracing approach, further allows for a transition of the beams into shadow zones. Thus, it is an attractive solution as compared to conventional ray tracing and provides more accurate results while maintaining the computational efficiency.

The Gaussian beam method associates with each ray a beam with a Gaussian intensity profile normal to the ray. A pair of differential equations that govern the beam-width and curvature are integrated along with the standard ray equations to compute the beam field in the vicinity of the central ray of the beam. This method avoids certain ray-tracing artifacts such as perfect shadows and infinite energy levels at caustics [82]. This technique is attractive for high frequency, range-dependent applications in which other approaches such as normal mode, fast field, and parabolic models might not be practical alternative. It is particularly useful in the modeling of deep water propagation where generally only a few rays significant.

2.3.2 Bellhop Software

Beam tracing tools simulate the UWA channel for given details of environment, the source and receiver characteristics, and carrier frequency. Bellhop software is an efficient gaussian beam tracing tool for two-dimensional analysis of an ocean environment freely available to public [84]. It was developed in 1987 by Porter and Bucker at the Space and Naval Warfare Systems Center in San Diego.

Bellhop software calculates the acoustic field by numerically integrating the ray

equations to trace the path of beams. The central ray of a beam follows the standard equation,

$$\frac{d}{ds}\left(\frac{1}{c(r,z)}\frac{dr}{ds}\right) = -\frac{1}{c^2(r,z)}\nabla c(r,z), \tag{11}$$

where r is the range and z is the depth using cylindrical coordinates, s is the arc-length and $c(r,z)$ is the speed of sound at a particular point [82].

The input to Bellhop is a file containing environmental information such as transmission frequency, water depth, source and receiver locations, SSP, number of beams to be used, the angle of launched beams, and top and bottom boundary conditions. The SSP is provided by the World Ocean Atlas (WOA) in the National Oceanic and Atmospheric Administration (NOAA) [85]. It contains information of the worldwide sound speed at different times of the year. The bathymetry data is taken from the General Bathymetric Chart of the Oceans (GEBCO) [86], a public database offering samples of the depth of the sea bottom with an angular spacing of 30 arc-seconds. Lastly, the type of bottom sediments is provided by The National Geophysical Data Center (NGDC) [87] from the NOAA provides a database that contains surficial sediment descriptions for over 36,000 seafloor samples worldwide.

Bellhop generates an output file which contains information about arrival time, arrival angle, pressure amplitude, number of surface and number of bottom interactions. The main steps in using the Bellhop software are summarized in Figure 7.

2.4 Channel Modeling with Bellhop Software

In this part, we consider a location in Aegean Sea for latitude of 38.5 °N and longitude 25.5 °E (see Figure 8) with the information of the sound speed in average of the year of 2012 and obtain the channel impulse response for the carrier frequency of 12 kHz. This will be used as our channel model in the rest of this thesis.

The source and the destination are located 6 km apart from each other. We assume

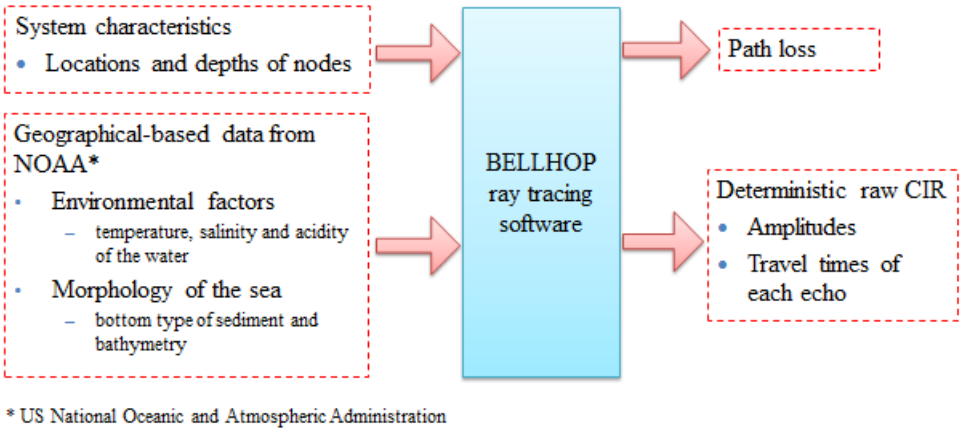

Figure 7: Input-output relationship of Bellhop software.

Figure 8: The simulation location in Aegean Sea.

Table 2: Simulation scenarios.

	Scenario I	**Scenario II**	**Scenario III**	**Scenario IV**
Source Depth	70 m	70 m	70 m	70 m
Relay 1 Depth	40 m	100 m	120 m	80 m
Relay 2 Depth	60 m	120 m	160 m	–
Relay 3 Depth	80 m	160 m	–	–
Relay 4 Depth	100 m	–	–	–
Destination Depth	70 m	150 m	150 m	70 m

the deployment of one, two, three or four relays which are located 2.5 km away from the source. We consider three different scenarios for which the depths of the source, relay and destination nodes are provided in Table 2. In Scenario I, the source and the destination both are located at a 70 m depth. Relays are located at the same distance from the source, but 20 m apart in depth from each other. In Scenarios II and III, the source and the destination, respectively are located at a depth of 70 m and 150 m. In Scenario IV, source, relay and destination are respectively located at a depth of 70 m, 80 m and 70 m.

In the following, we present some transmission loss contours to have some insight into UWA channel characteristics. In Figure 9, we provide the contours for Scenario I. In this figure, dark red represents the smallest transmission loss while dark blue represents the largest transmission loss. As observed from Figure 9, transmission loss effects differ significantly from what we typically observe in terrestrial RF systems. Specifically, there is not a constant decrease with respect to distance and the transmission loss for both underwater locations. Namely, they can be different from each other due to their depths even at the same distance. This is mainly as a result of the sound speed variation with depth which is also depicted in Figure 9.

Also, in order to clarify the relation between depth and transmission loss, we place the source at diverse depths as depicted in Figures 10, 11, and 12 and observe the

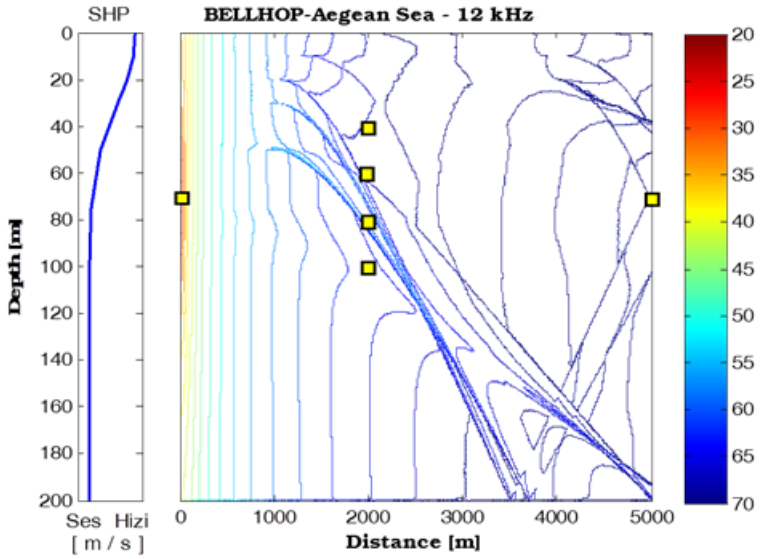

Figure 9: Average sound speed profile and transmission loss contours with respect to transmission range and depth. Nodes are located according to Scenario I.

results. In each figure, a different transmission loss contour is obtained due to the change in sound speed. Furthermore, we produce an another plot that shows the traveled paths for all the rays by using the output file (see Figure 13). The rays have different colors. These colors represent the strength of path between the source and destination and are helpful for visualizing the radiated energy distribution in the channel. A black ray is the weakest path while a red ray is the strongest path.

As detailed in the previous section, the Bellhop software produces arrival data which includes the amplitudes and travel times associated with each echo. This yields the deterministic raw channel impulse response (CIR) (see Figure 14).

The raw CIR should be further augmented with randomness due to fading. Let $\mathbf{h}'_{XY} = [h'_{XY}(1), \quad h'_{XY}(2), \quad .... \quad , h'_{XY}(L_{XY})]$ be the raw deterministic CIRs produced by the Bellhop software for the $X \rightarrow Y$ link. The transmission loss for the $X \rightarrow Y$ link can be calculated as $G_{XY} = \sum_{\ell=1}^{L_{XY}} E\left\{|h'_{XY}(\ell)|^2\right\}$. Dividing each element of $\mathbf{h}'_{XY}$ by G_{XY}, we find the normalized CIR as $\mathbf{h}_{XY} = [h_{XY}(1), \quad h_{XY}(2), \quad .... \quad , h_{XY}(L_{XY})]$

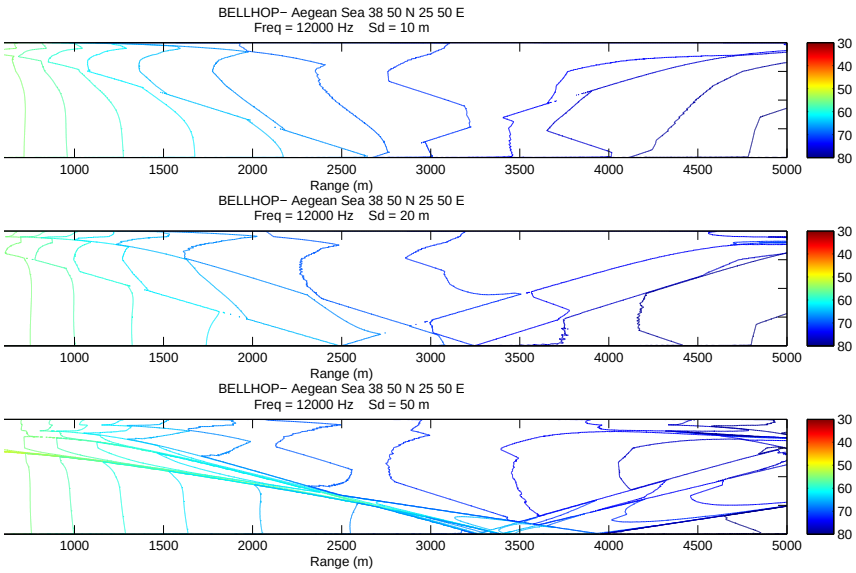

Figure 10: Ray tracing for distinct depth of source from 10 m to 50 m.

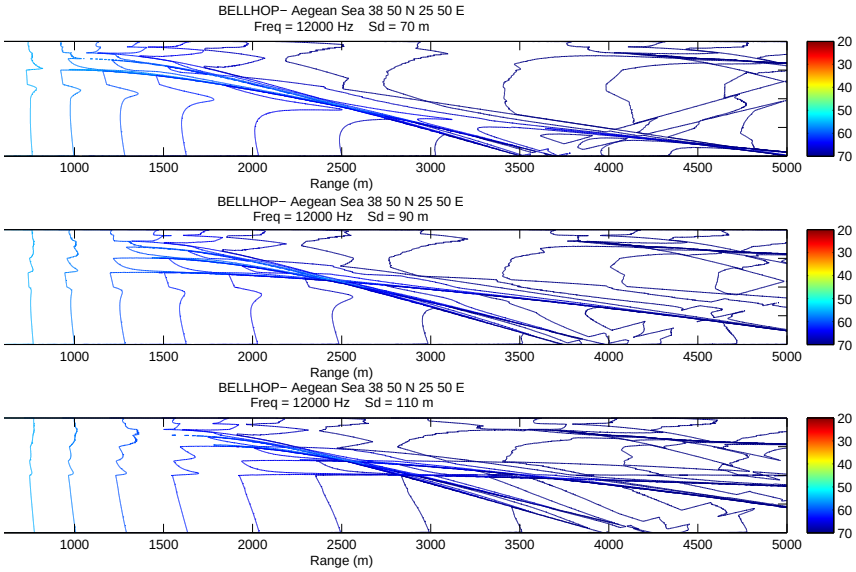

Figure 11: Ray tracing for distinct depth of source from 70 m to 110 m.

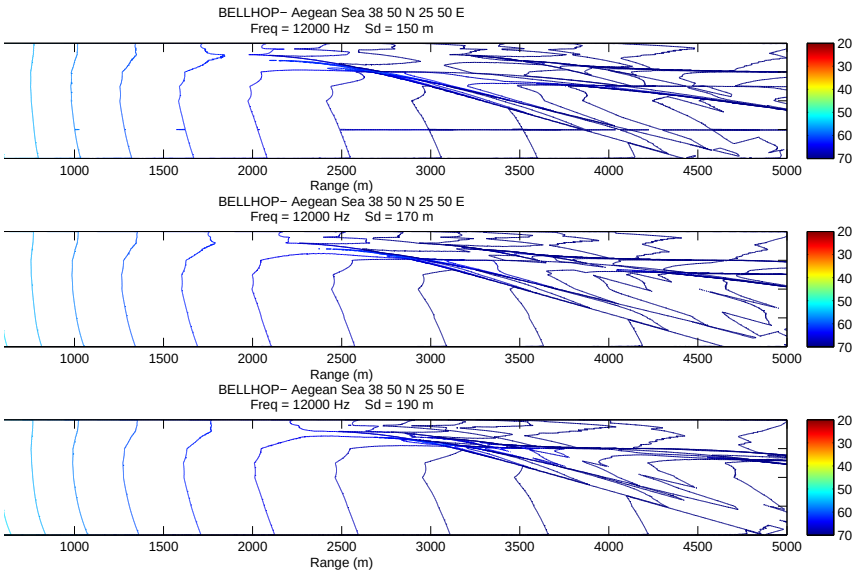

Figure 12: Ray tracing for distinct depth of source from 150 m to 190 m.

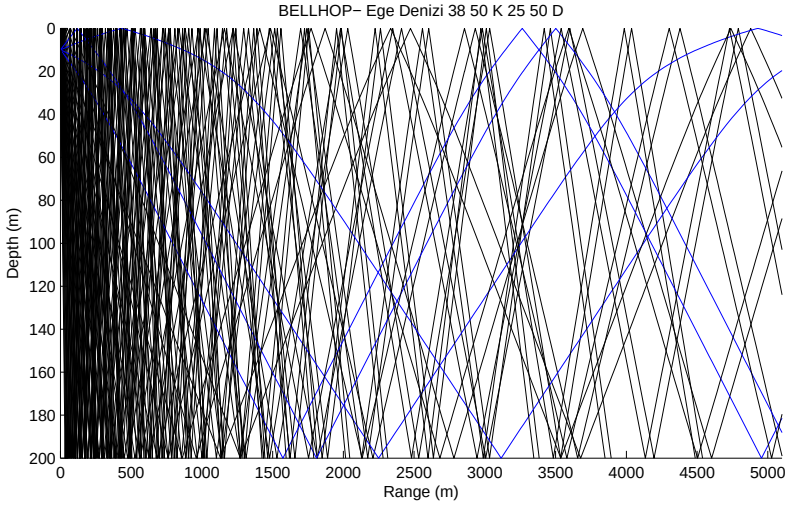

Figure 13: Traveled paths for all transmitted rays.

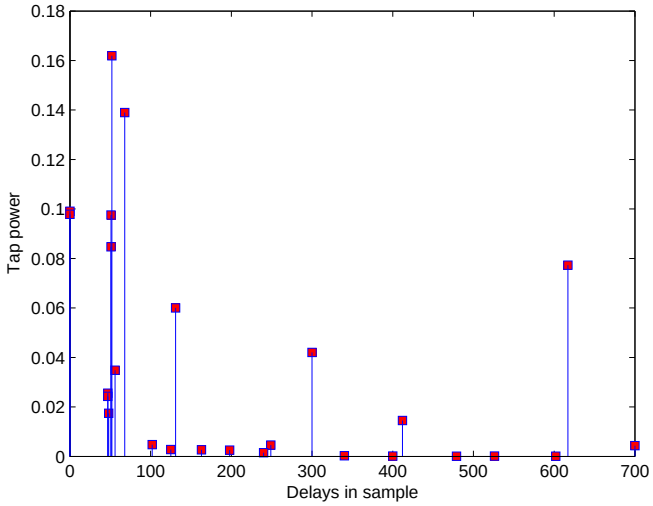

Figure 14: Deterministic raw channel impulse response.

with $\sum_{\ell}^{L_{XY}} \Omega_\ell = \sum_{\ell=1}^{L_{XY}} E\left\{|h_{XY}(\ell)|^2\right\} = 1$. Here, Ω_ℓ denotes the power of each coefficient, $\Omega_\ell = E\left\{|h_{XY}(\ell)|^2\right\}$. In our study, we assume Rician distribution to introduce the randomness on the tap coefficients. Thus, the channel coefficients, $h_{XY}(\ell)$, are independent and identically distributed (i.i.d) complex Gaussian random variables with mean $\mu_\ell/\sqrt{2}$ and variance σ_ℓ^2. They can be expressed as

$$h_{XY}(\ell) = \sqrt{\frac{\Omega_\ell k_\ell}{k_\ell + 1}}\left(\frac{1+j}{\sqrt{2}}\right) + \sqrt{\frac{\Omega_\ell}{k_\ell + 1}}\tilde{h}_{XY}(\ell), \tag{12}$$

where $\tilde{h}_{XY}(\ell)$ is complex Gaussian with zero mean and unit variance and also $\ell = 1,\ 2,\ \ldots,\ L_{XY}$.

Here, $\Omega_\ell = \mu_\ell^2 + 2\sigma_\ell^2$ and $k_\ell = \mu_\ell^2/2\sigma_\ell^2$ denote respectively, the power and the Rician constant over a period of one block transmission and vary independently from block to block. The corresponding channel frequency for a given block is given by

$$H_{XY}[k] = \sum_{\ell=1}^{L_{XY}} h_{XY}(\ell)\exp(-2j\pi\ell k/K), \tag{13}$$

where K is the number of subcarrier.

CHAPTER III

AAF RELAYING

3.1 Introduction

In this chapter, we consider an OFDM-based multi-relay UWA communication system along with RD protocol. We assume AaF relaying and deploy different selection criteria for relay selection [57, 58, 59, 60, 61] in our multi-relay system. The channel is modeled based on Bellhop software as explained in Chapter II. We present an extensive Monte Carlo simulation study and investigate the error rate performance of the system under consideration.

The chapter is organized as follows: In Section 3.2, we provide the transmission model. In Section 3.3, we present the relay selection rules under consideration. In Section 3.4, we discuss our simulation results and provide several insights into UWA communication system performance.

3.2 Transmission Model

We consider a multi-relay scenario where the source node S communicates to the destination node D with the assistance of relay(s). All terminals are half-duplex and equipped with a single transducer and hydrophone pair. The source, relay and destination nodes might be located at different depths. The relay(s) is (are) selected out of the N available relay nodes.

We assume RD cooperation protocol [38] with AaF relaying. The cooperative transmission takes place in two phases. In the first transmission phase, a bit stream is fed into a serial-to-parallel converter which maps them into modulation symbols

chosen from an MPSK constellation. After passing through inverse fast Fourier transform(IFFT), a cyclic prefix (CP) is inserted between OFDM symbols with $L_{CP} \geq max(L_{SR_n}, L_{R_nD}, L_{SD})$, $n = 1, 2, ..., N$ to prevent inter-block interference. Let the signal transmitted over the kth subcarrier be $X[k]$, $k = 1, 2, ..., K$. In the broadcasting phase, the received signals at the destination node and the relay nodes are given by

$$Y_{D,1}[k] = \sqrt{PG_{SD}}H_{SD}[k]X[k] + W_{D,1}[k], \tag{14}$$

$$Y_{R_n}[k] = \sqrt{PG_{SR_n}}H_{SR_n}[k]X[k] + W_{R_n}[k], \tag{15}$$

where G_{SD} and G_{SR_n} are respectively the transmission loss of $S \rightarrow D$ and $S \rightarrow R_n$ links, P denotes the transmit power and $n = 1, 2, ..., N$. In Eq. (14) and (15), $W_{D,1}[k]$ and $W_{R_n}[k]$ are the fast Fourier transform (FFT) of AWGN terms with zero mean and N_0 variance.

After removing the CP, the OFDM symbol is converted into parallel subcarrier symbols through FFT. The relay nodes perform a proper scaling of the subcarriers power to ensure that the power budget is not violated. Based on the predetermined relay selection criteria, one or more relays are engaged in the relaying phase. The selected relay(s) forward(s) the resulting signal(s) to the destination.

Mathematically, the relay node normalizes the signal at the respective received subcarrier by a factor of $E\left\{|Y_{R_n}[k]|^2\right\} = PG_{SR_n}|H_{SR_n}[k]|^2 + N_0$ before transmission. Therefore, the received signal at the destination during the relaying phase can be written as

$$Y_{D,2}[k] = \sqrt{\frac{G_{R_nD}G_{SR_n}}{PG_{SR_n}|H_{SR_n}[k]|^2 + N_0}}PH_{R_nD}[k]H_{SR_n}[k]X[k] + W'_{D,2}[k], \tag{16}$$

where $W'_{D,2}[k]$ represents the effective noise term and is conditionally Gaussian with

zero mean and variance of

$$\omega = \sqrt{\left(PG_{R_nD}|H_{R_nD}[k]|^2\right)/\left(PG_{SR_n}|H_{SR_n}[k]|^2 + N_0\right) + 1}. \tag{17}$$

After a proper normalization of Eq. (16), we can write the resulting normalized equation and Eq. (14) together in a matrix form as

$$\mathbf{Y} = \mathbf{H}X[k] + \mathbf{W}, \tag{18}$$

where $\mathbf{Y} = \begin{bmatrix} Y_{D,1}[k] & Y_{D,2}[k]/\omega \end{bmatrix}^T$, $\mathbf{W}$ (conditioned on $\mathbf{H}$) is AWGN with mean $E[\mathbf{W}|\mathbf{H}] = 0$ and covariance $E[\mathbf{W}\mathbf{W}^T|\mathbf{H}] = N_0\mathbf{I}_2$, and $\mathbf{H}$ is given by

$$\mathbf{H} = \begin{bmatrix} \sqrt{PG_{SD}}H_{SD}[k] \\ \frac{1}{\omega}\sqrt{\frac{G_{R_nD}G_{SR_n}}{PG_{SR_n}|H_{SR_n}[k]|^2+N_0}}PH_{R_nD}[k]H_{SR_n}[k] \end{bmatrix}. \tag{19}$$

At the destination, after removing CP and passing through the FFT, OFDM symbols received during the broadcasting and relaying phases are fed to a maximum ratio combining (MRC) detector.

3.3 Relay Selection Rules

We consider three relay selection rules which rely on a) maximization of SNR, b) minimization PoE, or c) maximization of capacity. Each rule is used in conjunction with different multi-carrier approaches [58, 59], namely

I. **All-subcarriers (AS) basis:** In this approach, to transmit the entire OFDM block to destination in the relaying phase, a single relay is used for all subcarriers. Its complexity and operational cost is the lowest.

II. **Per-subcarrier (PS) basis:** In this approach, for each subcarrier, a single relay is employed. Thus, the number of active relays in the relaying phase could be as high as N. Active relays transmit only the signals of their corresponding subcarrier and leave other subcarriers empty. It has the highest complexity.

III. **Subcarrier grouping (SG):** In this approach, the subcarriers are grouped, and a single relay is assigned for each group of subcarriers.

3.3.1 SNR-based Relay Selection

The instantaneous received SNRs in the links $S \rightarrow R_n$, $R_n \rightarrow D$, and $S \rightarrow D$ are denoted by $\gamma_{SR_n}^k$, $\gamma_{R_nD}^k$ and γ_{SD}^k, respectively. We consider only the indirect link SNR. This is because the direct link SNR, γ_{SD}^k, is the common term within the total received SNR at the destination. The instantaneous indirect link SNR is given by

$$\gamma_{SR_nD}^k = \frac{\gamma_{SR_n}^k \gamma_{R_nD}^k}{\gamma_{SR_n}^k + \gamma_{R_nD}^k + 1}, \tag{20}$$

where

$$\gamma_{SR_n}^k = \frac{|H_{SR_n}[k]|^2 P G_{SR_n}}{N_0}, \tag{21}$$

and

$$\gamma_{R_nD}^k = \frac{|H_{R_nD}[k]|^2 P G_{R_nD}}{N_0}. \tag{22}$$

In the maximization of SNR, we consider two selection rule: The first one, in a straightforward manner, chooses the relay with maximum SNR [57]. In the second one, we first determine the subcarrier with the worst SNR for each relay, and then choose the relay with the best SNR [61]. This is because overall bit error rate (BER) of OFDM is dominated by the performance of subcarrier with the worst SNR [88, 89].

3.3.1.1 Selection based on the Highest-SNR (hSNR)

In AS approach, all subcarriers' SNRs of each relay are summed up, and then, the relay along with highest SNR-sum are chosen. Therefore, the relay selection rule can be expressed as

$$\max_n \left\{ \sum_{k=1}^{K} \gamma_{SR_nD}^k \right\}. \tag{23}$$

In PS approach, our concentration is on individual subcarriers. So, we choose the relay which has the highest SNR for each subcarrier, i.e.,

$$\max_n \left\{ \gamma_{SR_nD}^k \right\}. \tag{24}$$

In SG approach, a group of $C(< K)$ subcarriers are taken into consideration in order to enhance the performance at cost of increasing the complexity and operational cost in the system. We select the relay which provides the largest combined indirect link SNR for this group, i.e.,

$$\max_{n} \left\{ \sum_{k=1}^{C} \gamma_{SR_nD}^{k} \right\}. \tag{25}$$

The explicit result is if $C = 1$, this approach is as same as the PS approach. Moreover, if $C = K$, it becomes the same as the AS approach.

3.3.1.2 Best-Of-Worst-based Relay Selection (BoW)

In the AS approach, for each relay, we first determine the subcarrier with the worst SNR. Then, we compare them and choose the relay with the best SNR among the worst SNRs. The relay selection rule can be therefore expressed as

$$\max_{n} \left\{ \min_{k} \left\{ \gamma_{SR_nD}^{k} \right\} \right\}, \tag{26}$$

where $k = 1, \ ..., \ K$.

PS approach is the same as the corresponding hSNR-based relay selection (in which the relay which provides the largest indirect link SNR for each subcarrier is chosen), i.e.

$$\max_{n} \left\{ \gamma_{SR_nD}^{k} \right\} \tag{27}$$

In SG approach, we find the smallest combined indirect link SNR for a group of $C(< K)$ subcarriers. The relay with the highest SNR among those with smallest SNRs is chosen for each corresponding group. Therefore, relay selection rule is expressed as

$$\max_{n} \left\{ \min_{k} \left\{ \gamma_{SR_nD}^{k} \right\} \right\} \tag{28}$$

as it is AS approach, but the difference from AS approach is $k = 1, \ ..., \ C$.

Table 3: Probability of error for different modulation orders [1].

$M = 2$	$Q\left(\sqrt{2\gamma^k_{SR_nD}}\right)$
$M = 4$	$Q\left(\sqrt{2\gamma^k_{SR_nD}}\right)\left[1 - 0.5Q\left(\sqrt{2\gamma^k_{SR_nD}}\right)\right]$
$M > 4$	$cQ\left(\sqrt{a\gamma^k_{SR_nD}}\right)$ $c = 2/\log_2 M$, $a = 2\log_2 M \sin^2(\pi/M)$ and M: constellation size.

3.3.2 PoE-based Relay Selection

The above selection criterion depends on the maximization of SNR. However, noting that PoE is a non-linear function of SNR, we consider another selection criteria based on the minimization of PoE.

In the AS approach, we calculate the conditional BER (given the fading realization) summed over all the subcarriers and choose the relay that provides the lowest sum. Therefore, the relay selection criteria for MPSK is given by

$$\min_n \left\{ \sum_{k=1}^{K} cQ\left(\sqrt{a\gamma^k_{SR_nD}}\right) \right\}. \tag{29}$$

where $Q(.)$ is the Gaussian-Q function, and based on the availability of CSI, c and a for MPSK are as explained in Table 3.

In the PS approach, we select the relay which provides the smallest conditional PoE for each subcarrier, i.e.,

$$\min_n \left\{ cQ(\sqrt{a\gamma^k_{SR_nD}}) \right\}. \tag{30}$$

In SG approach, we select the relay which provides the smallest combined conditional PoE for the group of $C(< K)$ subcarriers, i.e.,

$$\min_n \left\{ \sum_{k=1}^{C} cQ(\sqrt{a\gamma^k_{SR_nD}}) \right\}. \tag{31}$$

3.3.3 Capacity-based Relay Selection

Ergodic capacity is another non-linear function of SNR and, similar to PoE, can be used in relay selection [60]. In the AS approach, we calculate the combined indirect link capacity over all the subcarriers for each relay and choose the relay that provides the highest sum. Therefore, the relay selection rule can be expressed as

$$\max_{n} \left\{ \frac{1}{2K} \sum_{k=1}^{K} \log_2 \left(1 + \gamma_{SR_nD}^{k}\right) \right\}. \tag{32}$$

In PS approach, we select the relay which provides the maximum indirect link capacity for each subcarrier, i.e.,

$$\max_{n} \left\{ \frac{1}{2} \log_2 \left(1 + \gamma_{SR_nD}^{k}\right) \right\}. \tag{33}$$

In SG approach, we select the relay which provides the maximum indirect link capacity for a group of $C(< K)$ subcarriers, i.e.,

$$\max_{n} \left\{ \frac{1}{2C} \sum_{k=1}^{C} \log_2 \left(1 + \gamma_{SR_nD}^{k}\right) \right\}. \tag{34}$$

3.4 Simulation Results

In this section, we consider a cooperative UWA communication system with a carrier frequency of 12 kHz and bandwidth of 8 kHz at a location in Aegean Sea (Please see Figure 8 and related details in Chapter II). The number of subcarriers in OFDM implementation is 2048 and therefore the subcarrier bandwidth is approximately 3.9 Hz. The modulation scheme in cooperative transmission is BPSK.

In Figure 15, we illustrate the histograms of relay selection criteria in underwater for AS approach. To emphasize the difference of UWA communication from RF case, we also include the results for a terrestrial RF system in Figure 16. For RF simulation, we use a combined model of transmission loss and shadowing. The ratio of received to transmitted power in dB is given by

$$\frac{Pr}{Pt}\ (dB) = 10\log_{10} K - 10\gamma \log_{10} \frac{d}{d_0} + \psi_{dB}, \tag{35}$$

where ψ_{dB} is a Gauss-distributed random variable with mean zero and variance σ^2_{dB}, K is a constant transmission loss factor, and γ is transmission loss exponent [90].

In RF case, similar to Scenario I (in Table 2 of Chapter II), the source and the destination are located 6 km apart from each other. Four relays are 2.5 km away from the source and they are located on the same vertical line 20 m apart from each other. We assume $K = -31.54$ dB, $\sigma^2_{dB} = 3.65$ dB and $\gamma = 3.71$. As expected from RF propagation, all relays are selected in nearly close percentages of 25 % due to the same transmission loss values (see Figure 16). On the other hand, the histograms for UWA communication are strikingly different. As observed in Figure 15 for Scenario I, the third relay is selected most, followed by the second relay. The first and fourth relay are chosen with almost equal probability. These observations are consistent with the transmission loss experienced by each relay. It can be noticed from Figure 9 of Chapter II that the third relay experiences the lowest transmission loss (c.f., the third node is on ~ 50 dB transmission loss contours) while the first and fourth relay suffer the highest transmission loss (c.f., as indicated by ~ 65 dB transmission loss contours).

In Figure 17, we compare BER performance of AS, SG and PS approaches for BoW-based relay selection criteria with $N = 2$ and $N = 3$ relays (see Scenarios II and III in Table 2 of Chapter II). It is observed that the AS approach does not extract full diversity for the uncoded OFDM system under consideration since the whole OFDM signal is transmitted by the same relay. However, the PS approach extracts full spatial diversity of 3 for $N = 2$, and 4 for $N = 3$ at the cost of using up all the relays. Also, the performance of SG approach is between AS and PS approaches.

In Figure 18, we demonstrate the BER performance of hSNR-based, BoW-based, Capacity-based, and PoE-based relay selection criteria with AS, PS and SG approaches. We assume Scenario I in this figure. Deployed in conjunction with AS

and PS approaches, the performance of all relay selection criteria become nearly the same. As an intermediate and practical solution, the performance of SG approach lies between these two extreme cases. Deployed in conjunction with the SG approach, their performances differ from each other. At a BER rate of 10^{-4}, the performance improvement of PoE-based relay selection over hSNR and Capacity-based relay selection is about 1.2 dB and 0.6 dB, respectively for a group of 8 subcarriers (i.e. $C = 8$), while it has very similar performance with BoW-based relay selection.

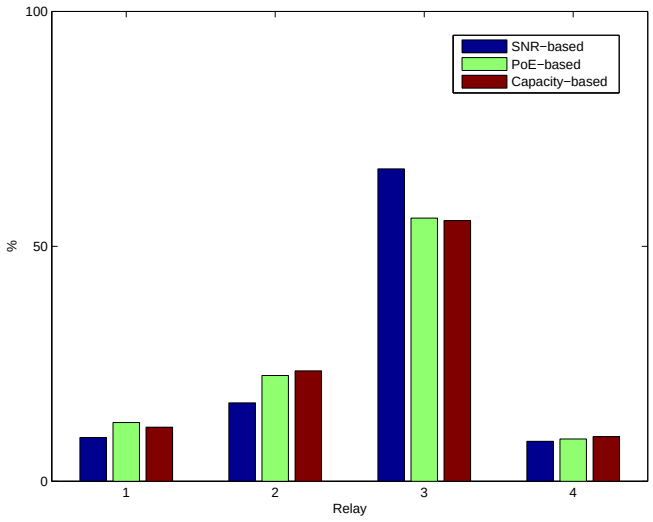

Figure 15: Histograms for UWA communication (Scenario I).

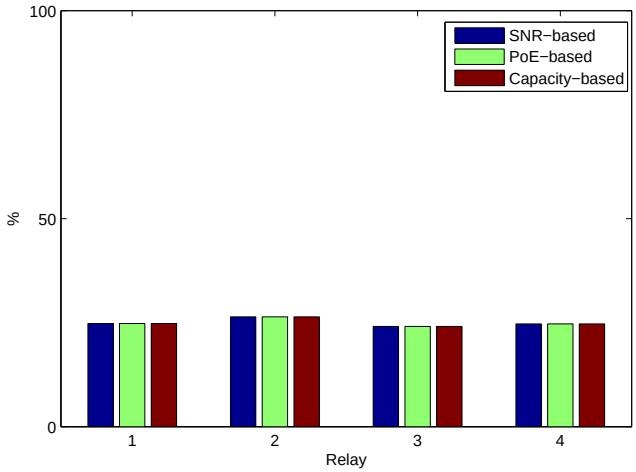

Figure 16: Histograms for terrestrial RF transmission.

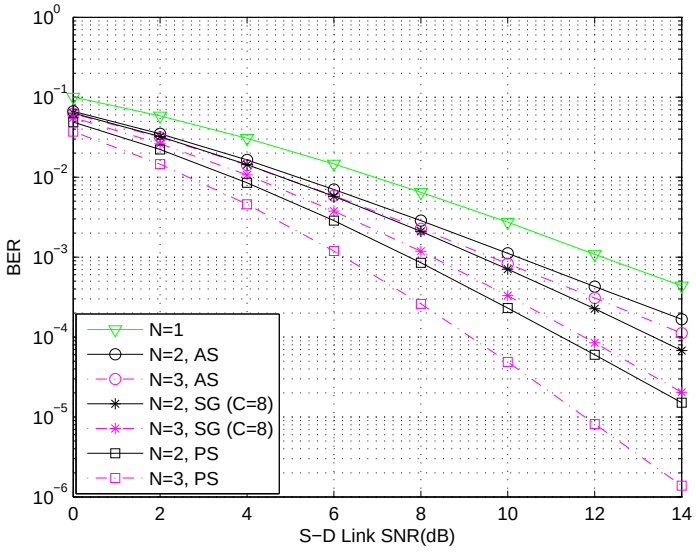

Figure 17: BER performance of BoW-based relay selection method for two and three relays (Scenario II and Scenario III).

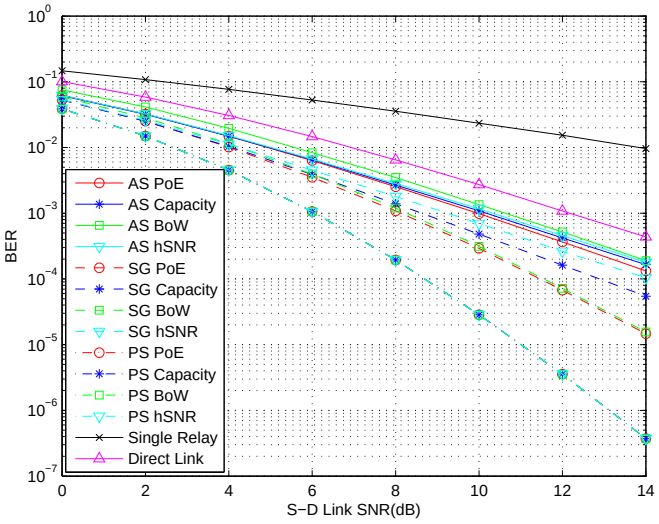

Figure 18: Comparison of BER performance for different relay selection methods (Scenario I).

CHAPTER IV

DAF RELAYING

4.1 Introduction

In the previous chapter, we have studied error rate performance of relay selection in underwater assuming AaF relaying. In this chapter, we consider DaF relaying as an alternative. We employ the same relay selection rules considered in Chapter III and consider only the AS approach which has the lowest complexity and operational cost.

The rest of the chapter is organized as follows. In Section 4.2 , we provide the transmission model. In Section 4.3, we present the relay selection rules. In Section 4.4, we present our simulation results.

4.2 Transmission Model

We consider a multi-relay scenario with N relay nodes. All nodes are half-duplex and equipped with a single transducer and hydrophone pair. We assume RD cooperation protocol. OFDM with properly designed cyclic prefix (i.e., assume a cyclic prefix that is long enough to accommodate the channel delay spread) is used to transform every link into K parallel channels, each at a different subcarrier experiencing frequency flat fading. Let the signal transmitted over the kth subcarrier be $X[k]$, $k = 1, 2, ..., K$. In the broadcasting phase, the received signals by the relays and destination at the kth subcarrier are given by

$$Y_{D,1}[k] = \sqrt{PG_{SD}}H_{SD}[k]X[k] + W_{D,1}[k], \tag{36}$$

$$Y_{R_n}[k] = \sqrt{PG_{SR_n}}H_{SR_n}[k]X[k] + W_{R_n}[k], \tag{37}$$

where P denotes the transmit power, G_{SD} and G_{SR_n} are respectively the transmission loss of $S \rightarrow D$ and $S \rightarrow R_n$ links, $n = 1, 2, ..., N$. In Eq. (36) and (37), $W_{D,1}[k]$ and $W_{R_n}[k]$ are the FFT of AWGN terms with zero mean and N_0 variance.

In the relaying phase, a DaF relay decodes the received signal and performs the error detection mechanism (i.e., CRC) in order to detect the potential decoding errors. If decoding is in error, the relay remains silent. If no decoding error is identified by the CRC, the relay re-modulate and forwards it to the destination. The received signal at the destination is given by

$$Y_{D,2}[k] = \sqrt{G_{R_nD}P}H_{R_nD}[k]\hat{X}[k] + W_{D,2}[k], \tag{38}$$

where $W_{D,2}[k]$ are the FFT of AWGN terms with zero mean and N_0 variance. OFDM symbols received during the broadcasting and relaying phases are then fed to a MRC detector at the destination node.

4.3 Relay Selection Rules

Since a relay is active only when the message is decoded correctly, we take into account only the performance of $R \rightarrow D$ indirect link in relay selection. Otherwise, destination only receives an information from the direct link of $S \rightarrow D$.

Relay selection criteria are summarized in Table 4. They are used with AS approach in which a single relay is used for all subcarriers.

4.4 Simulation Results

We consider a cooperative multi-carrier UWA communication system with the carrier frequency of 12 kHz and bandwidth of the 500 Hz. The number of subcarriers in OFDM implementation is 128 and therefore the subcarrier bandwidth is approximately 3.9 Hz. Other details on the simulation scenarios and assumptions are already provided in Chapter II.

Table 4: Relay selection criteria in DaF relaying.

hSNR based	$\max_n \left\{ \sum_{k=1}^{K} \gamma_{R_n D}^k \right\}$
BoW based	$\max_n \left\{ \min_k \left\{ \gamma_{R_n D}^k \right\} \right\}$
Capacity based	$\max_n \left\{ \frac{1}{2K} \sum_{k=1}^{K} \log_2 \left(1 + \gamma_{R_n D}^k\right) \right\}$
PoE based	$\min_n \left\{ \sum_{k=1}^{K} cQ(\sqrt{a\gamma_{R_n D}^k} \right\}$ where c and a are as defined in Chapter III

In Figure 19, we provide BER performance of hSNR-based method for $N = 2$ and $N = 3$ relays assuming Scenarios II and III (see Table 2 of Chapter II). Through increasing the number of relays, performance of the system improves around 1.8 dB at a BER rate of 10^{-3}.

In Figure 20, we demonstrate the BER performance of hSNR-based, BoW-based, PoE-based and Capacity based relay selection criteria in Scenario II. Albeit all methods show similar performance, PoE-based selection is the worst one. BoW-based relay selection method is best one at higher SNRs.

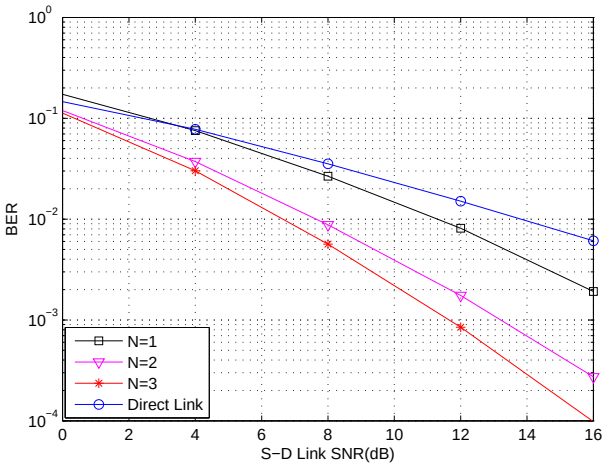

Figure 19: Performance of hSNR-based relay selection for two and three relays in conjunction with AS approach (Scenario II and III).

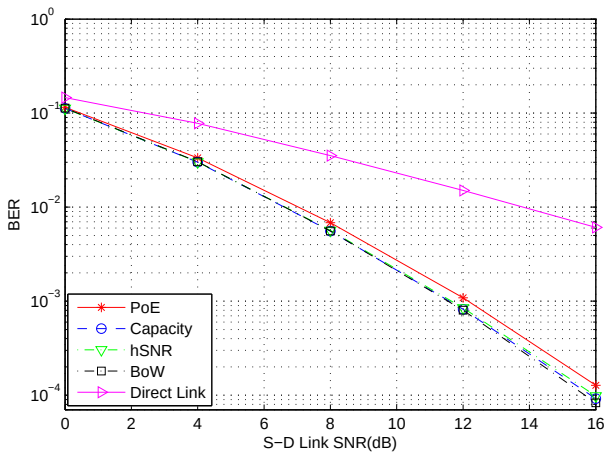

Figure 20: Performance of different relay selection criteria for three relays in conjunction with AS approach (Scenario II).

CHAPTER V

TWO-WAY RELAYING

5.1 Introduction

In this chapter, to mitigate the spectral loss in one-way communication, we consider a multi-carrier multi-relay UWA communication system operating in two-way mode. We take into consideration both conventional relaying in which all relay nodes participate in the relaying phase, and relay selection. We employ the similar relay selection rules considered in Chapter III such as SNR-based, PoE-based and Capacity-based relay selection criteria. Monte Carlo simulations are carried out to provide the error rate performance of the system.

The chapter is organized as follows. In Section 5.2, we present the transmission model. In Section 5.3, we discuss relay selection rules under consideration. In Section 5.4, we provide simulation results.

5.2 Transmission Model

We consider a two-way OFDM multi-relay network where two terminals communicate with the assistance of AaF relay(s) (see Figure 21 and 22). We assume that there is no direct link between the two terminals. All terminals operate in half-duplex mode and are equipped with a single transducer and hydrophone pair. BPSK modulation is deployed for cooperative transmission.

In the broadcasting phase, suppose that the terminals T_1 and T_2 exchange their data simultaneously in the first time slot. In the relaying phase, one of the relays is selected according to predetermined relay selection procedure in order to transmit this data. Then, the chosen relay amplifies its received signal properly and forwards it

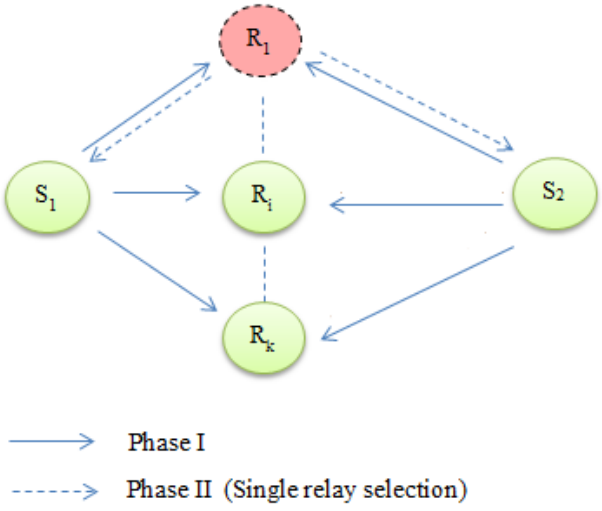

Figure 21: Two-way relaying with relay selection.

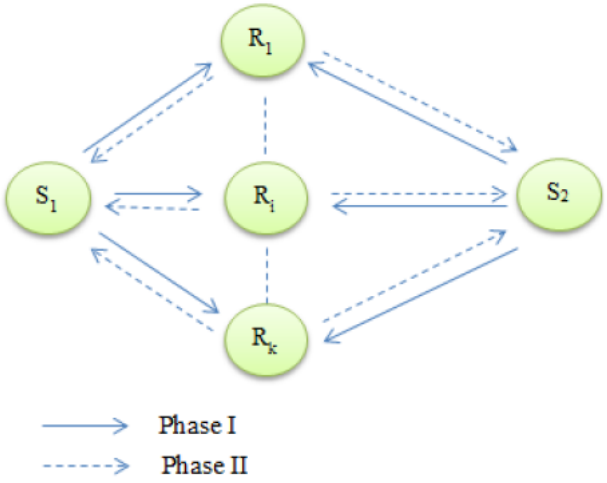

Figure 22: Conventional two-way relaying.

to both terminals. Based on the fact that each source has knowledge of its originally transmitted data, both T_1 and T_2 cancel their self-interference from the received signal to recover the data of other terminal. Let the signal transmitted by terminal T_p over the kth subcarrier be $X_p[k]$, $k = 1, 2, ..., K$, $p = 1, 2$. The received signal at the relay terminal R_i is given by

$$Y_{R_i}[k] = \sqrt{G_{T_1R_i}P}H_{T_1R_i}[k]X_1[k] + \sqrt{G_{T_2R_i}P}H_{T_2R_i}[k]X_2[k] + W_{R_i}[k], \tag{39}$$

where P denotes the transmit power, $G_{T_1R_i}$ and $G_{T_2R_i}$ are respectively the transmission loss of $T_1 \rightarrow R_i$ and $T_2 \rightarrow R_i$ links, , $i = 1, 2, ..., N$ and $W_{R_i}[k]$ is the FFT of AWGN term with zero mean and N_0 variance.

During the relaying phase, the selected relays transmit normalized version of their received signals. Assuming the channels between end terminals and relays are reciprocal (i.e., $H_{T_jR_i}[k] = H_{R_iT_j}[k]$), $j = 1, 2$, $i = 1, 2,$ $..., N$) the received signal at T_1 from R_i is given by

$$Y_{T_1R_i}[k] = \frac{\sqrt{G_{T_1R_i}P}H_{T_1R_i}[k]Y_{R_i}[k]}{\sqrt{G_{T_1R_i}P|H_{T_1R_i}[k]|^2 + G_{T_2R_i}P|H_{T_2R_i}[k]|^2 + N_0}} + W_{T_1R_i}[k] \tag{40}$$

where $W_{T_1R_i}[k]$ is the FFT of AWGN term with zero mean and N_0 variance.

After canceling the self-interference, the received signal at T_1 from R_i is given by

$$\begin{aligned} Y_{T_1R_i}[k] = &\frac{\sqrt{G_{T_1R_i}G_{T_2R_i}}PH_{T_1R_i}[k]H_{T_2R_i}[k]X_2[k]}{\sqrt{G_{T_1R_i}P|H_{T_1R_i}[k]|^2 + G_{T_2R_i}P|H_{T_2R_i}[k]|^2 + N_0}} + \\ &\frac{\sqrt{G_{T_1R_i}P}H_{T_1R_i}[k]W_{R_i}[k]}{\sqrt{G_{T_1R_i}P|H_{T_1R_i}[k]|^2 + G_{T_2R_i}P|H_{T_2R_i}[k]|^2 + N_0}} + W_{T_1R_i}[k]. \end{aligned} \tag{41}$$

Terminal T_1 normalizes the received signal in Eq. (5.3) with

$$\sqrt{\frac{G_{T_1R_i}P|H_{T_1R_i}[k]|^2}{G_{T_1R_i}P|H_{T_1R_i}[k]|^2 + G_{T_2R_i}P|H_{T_2R_i}[k]|^2 + N_0} + 1}. \tag{42}$$

This results in

$$Y_{T_1R_i}[k] = \sqrt{A_i}H_{T_1R_i}[k]H_{T_2R_i}[k]X_2[k] + W'_{T_1R_i}[k] \tag{43}$$

where $W'_{T_1R_i}[k]$ is the FFT of AWGN term with zero mean and N_0 variance and A_i is defined as

$$A_i = \frac{G_{T_1R_i}G_{T_2R_i}P^2}{G_{T_1R_i}P|H_{T_1R_i}[k]|^2 + (G_{T_1R_i}P|H_{T_1R_i}[k]|^2 + G_{T_2R_i}P|H_{T_2R_i}[k]|^2 + N_0)}. \quad (44)$$

Similarly at terminal T_2, the received signal after self-interference cancelation and normalization from R_i is given by

$$Y_{T_2R_i}[k] = \sqrt{B_i}H_{T_2R_i}[k]H_{T1R_i}[k]X_2[k] + W'_{T_2R_i}[k] \quad (45)$$

where $W'_{T_2R_i}[k]$ is the FFT of AWGN term with zero mean and N_0 variance and B_i is defined as

$$B_i = \frac{G_{T_2R_i}G_{T_1R_i}P^2}{G_{T_2R_i}P|H_{T_2R_i}[k]|^2 + (G_{T_1R_i}P|H_{T_1R_i}[k]|^2 + G_{T_2R_i}P|H_{T_2R_i}[k]|^2 + N_0)}. \quad (46)$$

5.3 Relay Selection Rules

5.3.1 SNR-based Relay Selection

This selection method relies on the maximization of the smaller of the received SNRs by two sources [91]. The received SNRs at both sources can be written as Eq. (47) and (48):

$$\gamma_{1,i}^k = \frac{G_{T_1R_i}G_{T2R_i}P^2|H_{T_1R_i}[k]|^2|H_{T_2R_i}[k]|^2}{N_0G_{T_1R_i}P|H_{T_1R_i}[k]|^2 + N_0(G_{T_1R_i}P|H_{T_1R_i}[k]|^2 + G_{T_2R_i}P|H_{T_2R_i}[k]|^2 + N_0)}, \quad (47)$$

$$\gamma_{2,i}^k = \frac{G_{T_2R_i}G_{T_1R_i}P^2|H_{T_2R_i}[k]|^2|H_{T_1R_i}[k]|^2}{N_0G_{T_2R_i}P|H_{T_2R_i}[k]|^2 + N_0(G_{T_1R_i}P|H_{T_1R_i}[k]|^2 + G_{T_2R_i}P|H_{T_2R_i}[k]|^2 + N_0)}, \quad (48)$$

In conjunction with AS, PS and SG approaches, SNR-based relay selection rules are provided in Table 5.

Table 5: SNR-based relay selection rules.

AS approach	$\max_i \left\{ \min \left\{ \sum_{k=1}^{K} \gamma_{1,i}^k, \sum_{k=1}^{K} \gamma_{2,i}^k \right\} \right\}$
PS approach	$\max_i \left\{ \min \left\{ \gamma_{1,i}^k, \gamma_{2,i}^k \right\} \right\}$
SG approach	$\max_i \left\{ \min \left\{ \sum_{k=1}^{C} \gamma_{1,i}^k, \sum_{k=1}^{C} \gamma_{2,i}^k \right\} \right\}$ where $C(< K)$

Table 6: PoE-based optimal relay selection rules.

	Optimal
AS approach	$\min_i \left\{ \sum_{k=1}^{K} \left(2Q\left(\sqrt{a\gamma_{1,i}^k}\right) + 2Q\left(\sqrt{a\gamma_{2,i}^k}\right) \right) \right\}$
PS approach	$\min_i \left\{ 2Q\left(\sqrt{a\gamma_{1,i}^k}\right) + 2Q\left(\sqrt{a\gamma_{2,i}^k}\right) \right\}$
SG approach	$\min_i \left\{ \sum_{k=1}^{C} \left(2Q\left(\sqrt{a\gamma_i^k}\right) + 2Q\left(\sqrt{a\gamma_{2,i}^k}\right) \right) \right\}$

5.3.2 PoE-based Relay Selection

We consider two selection criteria here. In the first one, a single relay which minimizes the sum symbol error rate (SER) of the two sources is selected to forward the received signals to both terminals. The second criteria takes into account that the sum SERs of two source nodes is typically dominated by the SER of the worst user and chooses the relay node which minimizes the maximum SER of two users. This is a suboptimal, yet low complexity solution [92]. Selection criteria with AS, PS and SG approaches are provided in Table 6 and 7.

5.3.3 Capacity-based Relay Selection

This selection method is based on the maximization of the achievable sum rate of two communicating nodes [93] and is provided in Table 8 for AS, PS and SG approaches.

Table 7: PoE-based suboptimal relay selection rules.

	Suboptimal
AS approach	$\min_i \left\{ \max \left\{ \sum_{k=1}^{K} 2Q\left(\sqrt{a\gamma_{1,i}^k}\right), \sum_{k=1}^{K} 2Q\left(\sqrt{a\gamma_{2,i}^k}\right) \right\} \right\}$
PS approach	$\min_i \left\{ \max \left\{ 2Q\left(\sqrt{a\gamma_{1,i}^k}\right), 2Q\left(\sqrt{a\gamma_i^k}\right) \right\} \right\}$
SG approach	$\min_i \left\{ \max \left\{ \sum_{k=1}^{C} 2Q\left(\sqrt{a\gamma_{1,i}^k}\right), \sum_{k=1}^{C} 2Q\left(\sqrt{a\gamma_{2,i}^k}\right) \right\} \right\}$

Table 8: Capacity-based relay selection rules.

AS approach	$\max_i \left\{ \frac{1}{2} \sum_{k=1}^{K} \left[\log_2(1+\gamma_{1,i}^k) + \log_2(1+\gamma_{2,i}^k) \right] \right\}$
PS approach	$\max_i \left\{ \frac{1}{2} \sum_{k=1}^{C} \left[\log_2(1+\gamma_{1,i}^k) + \log_2(1+\gamma_{2,i}^k) \right] \right\}$
SG approach	$\max_i \left\{ \frac{1}{2} \left[\log_2(1+\gamma_{1,i}^k) + \log_2(1+\gamma_{2,i}^k) \right] \right\}$

5.4 Simulation Results

We consider a cooperative multi-carrier multi-relay UWA communication system with the carrier frequency of 12 kHz and bandwidth of the 8 kHz. The number of subcarriers in OFDM implementation is 2048 and therefore the subcarrier bandwidth is approximately 3.9 Hz. Other details on the assumptions and scenarios in the simulations are already provide in Chapter II.

Figure 23 presents the SER performance of two-way conventional relaying for $N = 1, 2$ and 3. Both sources receive signals from all the relays and combine them using MRC. After that, SER is calculated at each source. For overall transmission, the system's SER is the summation of both these SERs. As it is seen that the diversity order enhances by the increase in the number of relays in both one-way and two-way relaying. For a fair comparison between the throughput of these two systems, we use QPSK modulation for one-way relaying simulations.

In Figure 24, we compare the SER performances of AS, and PS approaches for SNR-based relay selection criteria with $N = 2$ and $N = 3$ relays (see Scenarios II and III in Table 2 of Chapter II). PS approach is able to extract diversity about gain of 3 at the cost of using up all the relays, but not full diversity, while AS cannot extract diversity.

In Figure 25, we compare the SER performances of SNR-based, PoE-based and Capacity-based relay selection criteria with AS, PS and SG approaches in Scenario II. Deployed in conjunction with AS and PS approaches, the performance of all selection methods become nearly the same. SG approach lies between these two cases. In addition, performance improvement of PoE-based relay selection methods by using SG approach rather than AS approach is substantially more than the improvement in other selection methods such as SNR-based and Capacity-based relay selection criteria. Furthermore, the performances of optimal and suboptimal PoE-based relay selections are almost same and better than other two relay selection criteria in AS and SG approaches.

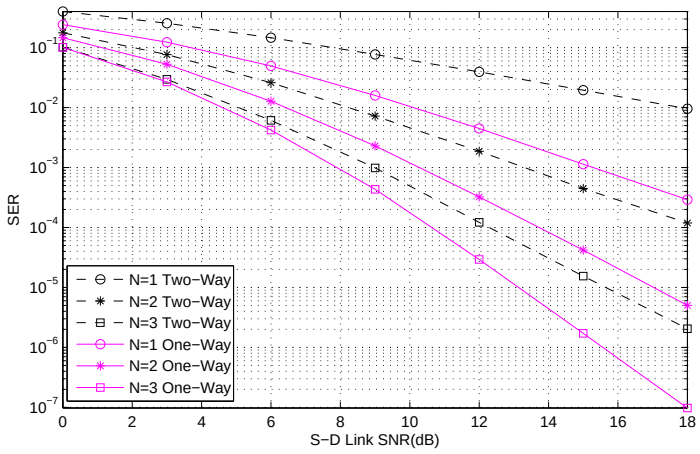

Figure 23: Performance results of two-way relaying and comparison with one-way relaying.

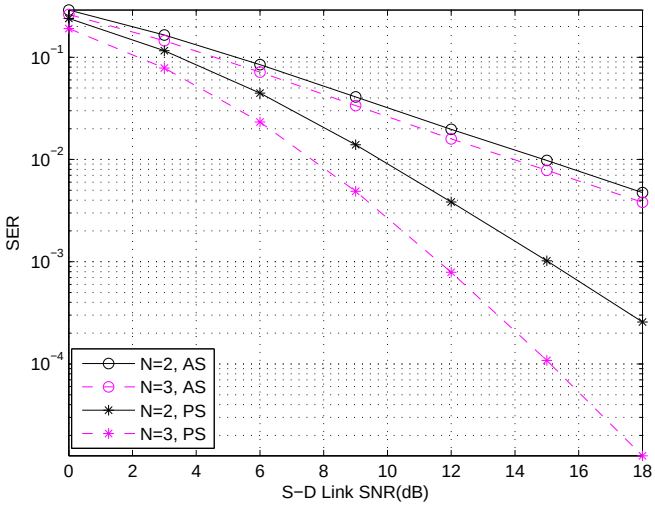

Figure 24: Performance of SNR-based relay selection for two-way relaying with two and three relays (Scenarios II and III).

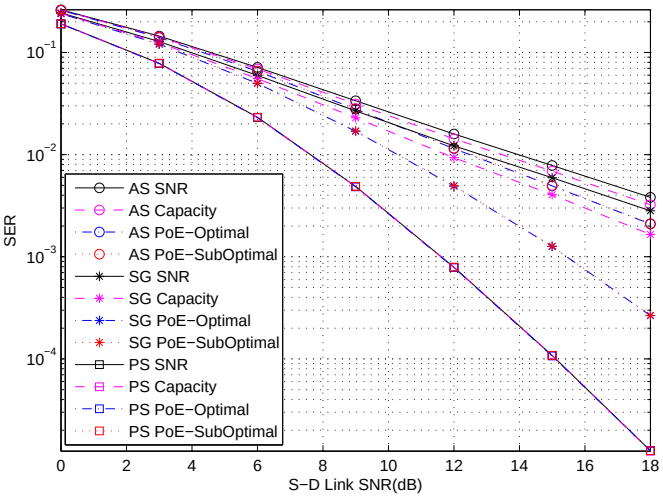

Figure 25: Performance of two-way relaying with different relay selection methods (Scenario II).

CHAPTER VI

SINGLE-CARRIER FREQUENCY DOMAIN EQUALIZATION (SC-FDE) FOR UWA COMMUNICATION

6.1 Introduction

In this chapter, we consider SC-FDE as an alternative to OFDM. SC-FDE provides a similar performance to OFDM with almost the same overall complexity. SC-FDE has common features with OFDM such as performing digital transmission blockwise and using FFT/IFFT operations. The main difference from OFDM is the displacement of IFFT operation from the transmitter to the receiver side (see Figure 26).

The chapter is organized as follows. In Section 6.2, we introduce the transmission model for SC-FDE. In Section 6.3, we present and discuss simulation results.

6.2 Transmission Model

We consider a single-relay scenario where the source node S communicates to the destination node D with the assistance of a relay R. All terminals are half-duplex and equipped with a single transducer and hydrophone pair. We adopt RD cooperation protocol and AaF relaying. QPSK linear modulation technique is used.

Let $\mathbf{X}^k$ denote a block of K modulated data symbols transmitted during the kth block transmission period. Last ℓ samples are appended as prefix of the block where ℓ is equal or greater than channel memory. This corrupted prefix is removed after passing through the multipath channel, therefore inter-block interference is avoided.

In broadcasting phase, the received signals by relay and destination are given by

$$\mathbf{r}_{\mathrm{R}}^k = \sqrt{PG_{\mathrm{SR}}}\mathbf{H}_{\mathrm{SR}}\mathbf{X}^k + \mathbf{n}_{\mathrm{R}}^k, \tag{49}$$

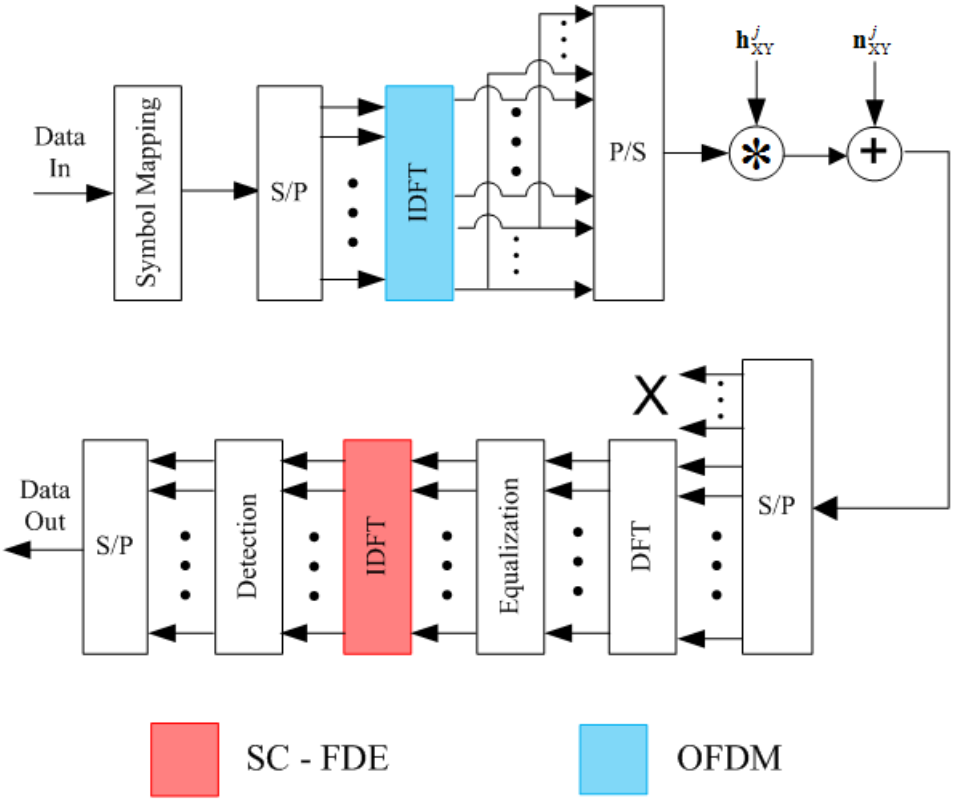

Figure 26: Block diagram of SC-FDE and OFDM digital communication systems.

$$\mathbf{r}_{\mathrm{D}}^{k} = \sqrt{PG_{\mathrm{SD}}}\mathbf{H}_{\mathrm{SD}}\mathbf{X}^{k} + \mathbf{n}_{\mathrm{D}}^{k} \tag{50}$$

where $\mathbf{n}_{\mathrm{D}}^{k}$ and $\mathbf{n}_{R}^{k}$ are the complex AWGN with zero mean and variance of $N_0/2$ per dimension. In addition, $\mathbf{H}_{SR}$ and $\mathbf{H}_{SD}$ are $K \times K$ circulant matrices with first column equal to the CIR appended by $(K - L_{SR} - 1)$ and $(K - L_{SD} - 1)$ zeros, respectively. Here, L_{SR} and L_{SD} denote corresponding channel memory lengths as detailed in Chapter II. Also, P is the transmit power, and G_{SD} and G_{SR} denote respectively the transmission loss of $S \to D$ and $S \to R$.

The relay terminal normalizes each entry of the received signal $\left[\mathbf{r}_{\mathrm{R}}^{k}\right]_{n}$, $n = 1, 2, \ldots, N$ by a factor of $E\left\{\left|\left[\mathbf{r}_{\mathrm{R}}^{k}\right]_{n}\right|^{2}\right\} = PG_{\mathrm{SR}} + N_0$ to ensure unit average energy and retransmits the signal during the second phase.

Therefore, the received signal at the destination terminal in the $(k+1)$th slot is given by

$$\mathbf{r}_{\mathrm{D}}^{k+1} = \sqrt{PG_{\mathrm{RD}}}\mathbf{H}_{\mathrm{RD}}\bar{\mathbf{r}}_{\mathrm{R}}^{k} + \mathbf{n}_{\mathrm{D}}^{k+1} \tag{51}$$

where $\bar{\mathbf{r}}_{\mathrm{R}}^{k}$ is the normalized received signal, $\mathbf{H}_{RD}$ is $K \times K$ circulant matrix with first column equal to the CIR appended by $(K - L_{RD} - 1)$ zeros and $\mathbf{n}_{\mathrm{D}}^{k+1}$ is the complex AWGN with zero mean and variance of $N_0/2$ per dimension.

Combining Eq. (51) and (49) we obtain,

$$\mathbf{r}_{\mathrm{D}}^{k+1} = \sqrt{\frac{G_{\mathrm{RD}}G_{\mathrm{SR}}}{PG_{\mathrm{SR}} + N_0}}P\mathbf{H}_{\mathrm{RD}}\mathbf{H}_{\mathrm{SR}}\mathbf{X}^{k} + \tilde{\mathbf{n}}_{\mathrm{D}}^{k+1} \tag{52}$$

where $\tilde{\mathbf{n}}_{\mathrm{D}}^{k+1}$ is the effective noise and given as

$$\tilde{\mathbf{n}}_{\mathrm{D}}^{k+1} = \sqrt{\frac{PG_{\mathrm{RD}}}{PG_{\mathrm{SR}} + N_0}}\mathbf{H}_{\mathrm{RD}}\mathbf{n}_{\mathrm{R}}^{k} + \mathbf{n}_{\mathrm{D}}^{k+1}. \tag{53}$$

Each entry of effective noise term $\tilde{\mathbf{n}}_{\mathrm{D}}^{k+1}$ (conditioned on $\mathbf{h}_{\mathrm{RD}}$) has zero mean and a variance of

$$E\left\{\left|\tilde{\mathbf{n}}_{\mathrm{D}}^{k+1}\right|_{n}^{2}\middle|\,\mathbf{h}_{\mathrm{RD}}\right\} = N_0\left(1 + \frac{PG_{\mathrm{RD}}}{PG_{\mathrm{SR}} + N_0}\sum_{m}^{L_{\mathrm{RD}}}\left|h_{\mathrm{RD}}\left(m\right)\right|^{2}\right) \text{ for } n = 1, \ldots, N. \tag{54}$$

The destination terminal normalizes the received signal by a factor of

$$\sqrt{1+\left(PG_{\mathrm{RD}}/(PG_{\mathrm{SR}}+N_0)\right)\sum_{m}^{L_{\mathrm{RD}}}\left|h_{\mathrm{RD}}(m)\right|^2}. \tag{55}$$

This result in

$$\bar{\mathbf{r}}_{\mathrm{D}}^{k+1}=\sqrt{\gamma_1}\mathbf{H}_{\mathrm{RD}}\mathbf{H}_{\mathrm{SR}}\mathbf{X}^k+\bar{\mathbf{n}}_{\mathrm{D}}^{k+1} \tag{56}$$

where $\bar{\mathbf{n}}_{\mathrm{D}}^{k+1}$ is complex Gaussian with zero mean and variance of $N_0/2$ per dimension and γ_1 is defined as

$$\gamma_1=\frac{\left(PG_{\mathrm{SR}}/N_0\right)PG_{\mathrm{RD}}}{1+PG_{\mathrm{SR}}/N_0\ +\left(PG_{\mathrm{RD}}/N_0\right)\sum_{m}^{L_{\mathrm{RD}}}\left|h_{\mathrm{RD}}(m)\right|^2}. \tag{57}$$

The received signals in Eq. (56) and (50) are transferred to frequency domain by multiplying discrete Fourier transform (DFT) matrix,

$$\mathbf{R}_{SC}^{k}=\mathbf{Q}\mathbf{r}_{D}^{k}=\sqrt{PG_{SD}}\mathbf{Q}\mathbf{H}_{SD}\mathbf{X}^k+\mathbf{Q}\mathbf{n}_{SD}^{k}, \tag{58}$$

$$\mathbf{R}_{SC}^{k+1}=\mathbf{Q}\bar{\mathbf{r}}_{D}^{k+1}=\sqrt{\gamma_1}\mathbf{Q}\mathbf{H}_{RD}\mathbf{H}_{SR}\mathbf{X}^k+\mathbf{Q}\bar{\mathbf{n}}_{SD}^{k+1} \tag{59}$$

where DFT matrix has the elements of $[\mathbf{Q}]_{k,l}=\left(1/\sqrt{K}\right)\exp\left(-j2\pi kl/K\right)$. Exploiting the circulant structure of the channel matrices, we have $\mathbf{H}_{SD}=\mathbf{Q}^H\mathbf{\Lambda}_{SD}\mathbf{Q}$, $\mathbf{H}_{SR}=\mathbf{Q}^H\mathbf{\Lambda}_{SR}\mathbf{Q}$ and $\mathbf{H}_{RD}=\mathbf{Q}^H\mathbf{\Lambda}_{RD}\mathbf{Q}$ where $\mathbf{\Lambda}_{SD}$, $\mathbf{\Lambda}_{SR}$ and $\mathbf{\Lambda}_{RD}$ are diagonal matrices whose (n,n) elements are equal to the nth DFT coefficients of $\mathbf{h}_{SD}$, $\mathbf{h}_{SR}$ and $\mathbf{h}_{RD}$. The received signal over two time slots after passing through DFT block can be written in a matrix format as

$$\begin{bmatrix}\mathbf{Q}\mathbf{r}_{\mathrm{D}}^{k}\\ \mathbf{Q}\bar{\mathbf{r}}_{\mathrm{D}}^{k+1}\end{bmatrix}=\underbrace{\begin{bmatrix}\sqrt{PG_{\mathrm{SD}}}\mathbf{\Lambda}_{\mathrm{SD}}\\ \sqrt{\gamma_1}\mathbf{\Lambda}_{\mathrm{RD}}\mathbf{\Lambda}_{\mathrm{SR}}\end{bmatrix}}_{\Upsilon}\mathbf{Q}\mathbf{X}^k+\begin{bmatrix}\mathbf{Q}\mathbf{n}_{\mathrm{D}}^{k}\\ \mathbf{Q}\bar{\mathbf{n}}_{\mathrm{D}}^{k+1}\end{bmatrix}. \tag{60}$$

MRC combining scheme for this cooperation is done by multiplying Eq. (60) with

$$\mathbf{\Gamma}=\left(\gamma_1|\mathbf{\Lambda}_{\mathrm{RD}}|^2|\Lambda_{\mathrm{SR}}|^2+PG_{\mathrm{SD}}|\mathbf{\Lambda}_{\mathrm{SD}}|^2\right)^{-1/2}\Upsilon^H. \tag{61}$$

The resulting output input relation can be written as

$$\mathbf{R}_{\mathrm{SC}} = \sqrt{\gamma_1 |\mathbf{\Lambda}_{\mathrm{RD}}|^2 |\Lambda_{\mathrm{SR}}|^2 + PG_{\mathrm{SD}} |\mathbf{\Lambda}_{\mathrm{SD}}|^2} \mathbf{Q}\mathbf{X}^k + \mathbf{N} \tag{62}$$

where $\mathbf{N}$ is a noise vector with each entry is Gaussian with zero mean and variance of $N_0/2$ per dimension.

6.3 Simulation Results

In this section, we present a simulation study to compare the performance of SC-FDE and uncoded OFDM. For OFDM, we consider a carrier frequency of 12 kHz and bandwidth of 8 kHz. For SC-FDE, we consider a carrier frequency of 12 kHz and bandwidth of 1 kHz. The number of symbols in a block is 2048. Therefore for OFDM the subcarrier bandwidth is approximately 3.9 Hz and for SC-FDE symbol duration is 1 msn.

In Figure 27, we compare the BER performance of SC-FDE and uncoded OFDM systems along with MMSE or ZF equalizers. It is observed that SC-FDE outperforms uncoded OFDM. In SC-FDE, decisions are made in the time-domain whereas in OFDM, decisions are made in the frequency-domain. Thanks to use of IFFT operation at the receiver in SC-FDE the noise contributions of all of the individual subcarriers is spread; therefore, narrowband notches in the channel frequency response have only a small impact on error probability [94, 95]. So, the overall performance is enhanced, and partial diversity is extracted while uncoded OFDM whose diversity order is limited to one, see, e.g., [96, 97]. It is further observed that in the SC-FDE system, MMSE equalizer outperforms ZF equalizer due to reduction of noise enhancement, whereas there is no difference for uncoded OFDM [94].

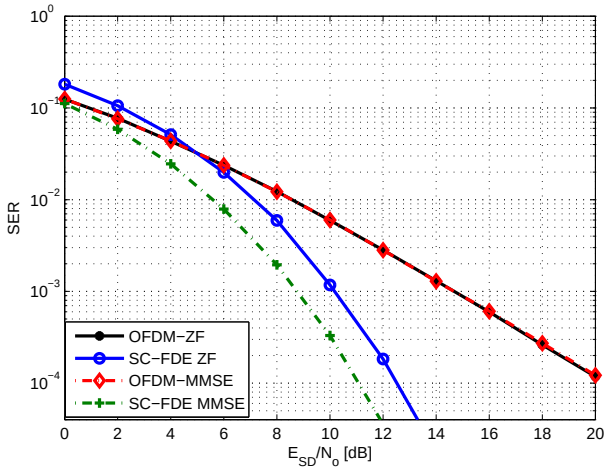

Figure 27: The performance comparison of uncoded OFDM and SC-FDE under consideration of MMSE and ZF equalizers (Scenario IV).

CHAPTER VII

CONCLUSIONS

Cooperative communication permits nodes in a wireless network to share their resources through distributed transmission unlike conventional point-to-point communications. In this thesis, we have presented a comprehensive performance analysis for cooperative UWA communication systems and investigated the performance of relay selection in underwater for multi-carrier and single-carrier systems. For a realistic channel characterization, we have considered an aggregate channel which combines the effect of large-scale transmission loss and small-scale fading and employed a ray-tracing based underwater propagation software. Through the deployment of Bellhop software, we have been reflected the characteristics of an underwater geographical location on the transmission loss and end-to-end system performance.

We have started with the analysis of OFDM-based multi-carrier multi-relay cooperative UWA communication system operating in both AaF and DaF relaying modes. We have adopted relay selection criteria which rely either on the maximization of SNR, the minimization of PoE, or the maximization of capacity for relay selection. These are utilized in conjunction with diverse approaches such as PS, AS, or SG. Our simulation results for UWA communication systems have reflected strikingly different results from terrestrial RF systems as a result of the effect of sound speed profile on the transmission loss of different nodes located at the same distance but different depths.

In the second part of research, to increase the spectral efficiency, we have considered two-way relaying in comparison with one-way communication. The SER performances of diverse relay selection rules along with different approaches are further

discussed. Our simulation results have demonstrated that the PoE-based methods outperform their competitors.

In the final part, we have considered SC-FDE as an alternative OFDM in a cooperative UWA communication system. We have shown that SC-FDE yields better performance than uncoded OFDM through spreading out the effects of deep nulls in the channel frequency response by using IFFT operation. Also, a comparison between two distinct linear equalization techniques like MMSE and ZF is provided. ZF performs worse than MMSE due to noise enhancement.

7.1 Future Works

Throughout this study, perfect channel estimation has been assumed. However, our work can be extended by taking into account of channel estimation problem in UWA communication systems. On the other hand, motion creates an extreme Doppler effect which has to be handled carefully. Thus, Doppler effect compensation can be though as an another possible research venue. Furthermore, optimization of system parameters and relays' location can be considered in order to improve the overall system performance.

Bibliography

[1] J. Proakis, *Digital communications*. McGraw-Hill, 2001.

[2] M. Stojanovic and J. Preisig, "Underwater acoustic communication channels: Propagation models and statistical characterization," *Communications Magazine, IEEE*, vol. 47, no. 1, pp. 84–89, 2009.

[3] W. Chen and F. Yanjun, "Physical layer design consideration for underwater acoustic sensor networks," in *Computer Science and Information Technology (ICCSIT), 2010 3rd IEEE International Conference on*, vol. 9, pp. 606–609, IEEE, 2010.

[4] K. Nagothu, *New paradigms for underwater communication*. ProQuest, 2009.

[5] L. Lanbo, Z. Shengli, and C. Jun-Hong, "Prospects and problems of wireless communication for underwater sensor networks," *Wireless Communications and Mobile Computing*, vol. 8, no. 8, pp. 977–994, 2008.

[6] X. Lurton, *Underwater acoustics: an introduction*. Springer, 2002.

[7] A. Quazi and W. Konrad, "Underwater acoustic communications," *Communications Magazine, IEEE*, vol. 20, no. 2, pp. 24–30, 1982.

[8] M. Stojanovic, "Recent advances in high-speed underwater acoustic communications," *Oceanic Engineering, IEEE Journal of*, vol. 21, no. 2, pp. 125–136, 1996.

[9] M. Suzuki, T. Sasaki, and T. Tsuchiya, "Digital acoustic image transmission system for deep-sea research submersible," in *OCEANS'92.'Mastering the Oceans Through Technology'. Proceedings.*, vol. 2, pp. 567–570, IEEE, 1992.

[10] G. Ayela and J. Coudeville, "Tiva: A long range, high baud rate image/data acoustic transmission system for underwater applications," in *Proc. Underwater Defence Technol. Conf*, p. 1991, 1991.

[11] A. Goalic, J. Labat, J. Trubuil, S. Saoudi, and D. Rioualen, "Toward a digital acoustic underwater phone," in *OCEANS'94.'Oceans Engineering for Today's Technology and Tomorrow's Preservation.'Proceedings*, vol. 3, pp. III–489, IEEE, 1994.

[12] M. Stojanovic, J. Catipovic, and J. Proakis, "Phase-coherent digital communications for underwater acoustic channels," *Oceanic Engineering, IEEE Journal of*, vol. 19, no. 1, pp. 100–111, 1994.

[13] M. Stojanovic, L. Freitag, and M. Johnson, "Channel-estimation-based adaptive equalization of underwater acoustic signals," in *OCEANS'99 MTS/IEEE. Riding the Crest into the 21st Century*, vol. 2, pp. 590–595, IEEE, 1999.

[14] M. Lopez and A. Singer, "A dfe coefficient placement algorithm for sparse reverberant channels," *Communications, IEEE Transactions on*, vol. 49, no. 8, pp. 1334–1338, 2001.

[15] C. Carbonelli and U. Mitra, "A simple sparse channel estimator for underwater acoustic channels," in *OCEANS 2007*, pp. 1–6, IEEE, 2007.

[16] W. Li and J. Preisig, "Estimation of rapidly time-varying sparse channels," *Oceanic Engineering, IEEE Journal of*, vol. 32, no. 4, pp. 927–939, 2007.

[17] J. Tao, Y. Zheng, C. Xiao, T. Yang, W. Yang, and A. Swami, "Channel equalization for single carrier mimo underwater acoustic communications," *EURASIP Journal on Advances in Signal Processing*, vol. 2010, 2010.

[18] Y. Zheng, C. Xiao, T. Yang, and W. Yang, "Frequency-domain channel estimation and equalization for shallow-water acoustic communications," *Physical Communication*, vol. 3, no. 1, pp. 48–63, 2010.

[19] E. Sozer, J. Proakis, and F. Blackmon, "Iterative equalization and decoding techniques for shallow water acoustic channels," in *OCEANS, 2001. MTS/IEEE Conference and Exhibition*, vol. 4, pp. 2201–2208, IEEE, 2001.

[20] F. Blackmon, E. Sozer, and J. Proakis, "Iterative equalization, decoding, and soft diversity combining for underwater acoustic channels," in *OCEANS'02 MTS/IEEE*, vol. 4, pp. 2425–2428, IEEE, 2002.

[21] T. Oberg, B. Nilsson, N. Olofsson, M. Nordenvaad, and E. Sangfelt, "Underwater communication link with iterative equalization," in *OCEANS 2006*, pp. 1–6, IEEE, 2006.

[22] J. Choi, R. Drost, A. Singer, and J. Preisig, "Iterative multi-channel equalization and decoding for high frequency underwater acoustic communications," in *Sensor Array and Multichannel Signal Processing Workshop, 2008. SAM 2008. 5th IEEE*, pp. 127–130, IEEE, 2008.

[23] J. Zhang and Y. Zheng, "Frequency-domain turbo equalization with soft successive interference cancellation for single carrier mimo underwater acoustic communications," *Wireless Communications, IEEE Transactions on*, vol. 10, no. 9, pp. 2872–2882, 2011.

[24] J. Tao, Y. Zheng, C. Xiao, and T. Yang, "Robust mimo underwater acoustic communications using turbo block decision-feedback equalization," *Oceanic Engineering, IEEE Journal of*, vol. 35, no. 4, pp. 948–960, 2010.

[25] S. Coatelan and A. Glavieux, "Design and test of a multicarrier transmission system on the shallow water acoustic channel," in *OCEANS'94.'Oceans Engineering for Today's Technology and Tomorrow's Preservation.'Proceedings*, vol. 3, pp. III–472, IEEE, 1994.

[26] M. Chitre, S. Ong, and J. Potter, "Performance of coded ofdm in very shallow water channels and snapping shrimp noise," in *OCEANS, 2005. Proceedings of MTS/IEEE*, pp. 996–1001, IEEE, 2005.

[27] A. Morozov and J. Preisig, "Underwater acoustic communications with multi-carrier modulation," in *OCEANS 2006*, pp. 1–6, IEEE, 2006.

[28] B. Li, J. Huang, S. Zhou, K. Ball, M. Stojanovic, L. Freitag, and P. Willett, "Mimo-ofdm for high-rate underwater acoustic communications," *Oceanic Engineering, IEEE Journal of*, vol. 34, no. 4, pp. 634–644, 2009.

[29] Z. Wang, S. Zhou, J. Preisig, K. Pattipati, and P. Willett, "Clustered adaptation for estimation of time-varying underwater acoustic channels," *Signal Processing, IEEE Transactions on*, vol. 60, no. 6, pp. 3079–3091, 2012.

[30] Z. Wang, S. Zhou, J. Catipovic, and P. Willett, "Parameterized cancellation of partial-band partial-block-duration interference for underwater acoustic ofdm," in *Proceedings of the Sixth ACM International Workshop on Underwater Networks*, p. 3, ACM, 2011.

[31] S. Roy, T. Duman, L. Ghazikhanian, V. McDonald, J. Proakis, and J. Zeidler, "Enhanced underwater acoustic communication performance using space-time coding and processing," in *OCEANS'04. MTTS/IEEE TECHNO-OCEAN'04*, vol. 1, pp. 26–33, IEEE, 2004.

[32] M. Stojanovic, "Mimo-ofdm over underwater acoustic channels," in *Signals, Systems and Computers, 2009 Conference Record of the Forty-Third Asilomar Conference on*, pp. 605–609, IEEE, 2009.

[33] Y. Emre, V. Kandasamy, T. Duman, P. Hursky, and S. Roy, "Multi-input multi-output ofdm for shallow-water uwa communications," *Journal of the Acoustical Society of America*, vol. 123, no. 5, p. 3891, 2008.

[34] R. Ormondroyd, "A robust underwater acoustic communication system using ofdm-mimo," in *OCEANS 2007-Europe*, pp. 1–6, IEEE, 2007.

[35] A. Sendonaris, E. Erkip, and B. Aazhang, "User cooperation diversity. part I. system description," *Communications, IEEE Transactions on*, vol. 51, no. 11, pp. 1927–1938, 2003.

[36] E. Van Der Meulen, "Three-terminal communication channels," *Advances in applied Probability*, pp. 120–154, 1971.

[37] T. Cover and A. Gamal, "Capacity theorems for the relay channel," *Information Theory, IEEE Transactions on*, vol. 25, no. 5, pp. 572–584, 1979.

[38] J. Laneman, D. Tse, and G. Wornell, "Cooperative diversity in wireless networks: Efficient protocols and outage behavior," *Information Theory, IEEE Transactions on*, vol. 50, no. 12, pp. 3062–3080, 2004.

[39] J. Laneman and G. Wornell, "Distributed space-time-coded protocols for exploiting cooperative diversity in wireless networks," *Information Theory, IEEE Transactions on*, vol. 49, no. 10, pp. 2415–2425, 2003.

[40] R. Nabar, H. Bolcskei, and F. Kneubuhler, "Fading relay channels: Performance limits and space-time signal design," *Selected Areas in Communications, IEEE Journal on*, vol. 22, no. 6, pp. 1099–1109, 2004.

[41] H. Ochiai, P. Mitran, and V. Tarokh, "Variable-rate two-phase collaborative communication protocols for wireless networks," *Information Theory, IEEE Transactions on*, vol. 52, no. 9, pp. 4299–4313, 2006.

[42] M. Uysal and M. Fareed, "Cooperative diversity systems for wireless communication," *INFORMATION AND CODING THEORY*, 2008.

[43] F. Onat, Y. Fan, H. Yanikomeroglu, and H. Poor, "Threshold-based relay selection for detect-and-forward relaying in cooperative wireless networks," *EURASIP Journal on Wireless Communications and Networking*, vol. 2010, p. 43, 2010.

[44] H. Mheidat and M. Uysal, "Impact of receive diversity on the performance of amplify-and-forward relaying under aps and ips power constraints," *Communications Letters, IEEE*, vol. 10, no. 6, pp. 468–470, 2006.

[45] K. Hwang, Y. Ko, and M. Alouini, "Performance analysis of two-way amplify and forward relaying with adaptive modulation," in *Personal, Indoor and Mobile Radio Communications, 2009 IEEE 20th International Symposium on*, pp. 2340–2344, IEEE, 2009.

[46] B. Rankov and A. Wittneben, "Spectral efficient signaling for half-duplex relay channels," in *Signals, Systems and Computers, 2005. Conference Record of the Thirty-Ninth Asilomar Conference on*, pp. 1066–1071, IEEE, 2005.

[47] Y. Han, S. Ting, C. Ho, and W. Chin, "High rate two-way amplify-and-forward half-duplex relaying with ostbc," in *Vehicular Technology Conference, 2008. VTC Spring 2008. IEEE*, pp. 2426–2430, IEEE, 2008.

[48] T. Unger and A. Klein, "Maximum sum rate of non-regenerative two-way relaying in systems with different complexities," in *Personal, Indoor and Mobile Radio Communications, 2008. PIMRC 2008. IEEE 19th International Symposium on*, pp. 1–6, IEEE, 2008.

[49] T. Cui, T. Ho, and J. Kliewer, "Memoryless relay strategies for two-way relay channels," *Communications, IEEE Transactions on*, vol. 57, no. 10, pp. 3132–3143, 2009.

[50] M. Stojanovic, "Capacity of a relay acoustic channel," in *OCEANS 2007*, pp. 1–7, IEEE, 2007.

[51] C. Carbonelli and U. Mitra, "Cooperative multihop communication for underwater acoustic networks," in *Proceedings of the 1st ACM international workshop on Underwater networks*, pp. 97–100, ACM, 2006.

[52] M. Vajapeyam, S. Vedantam, U. Mitra, J. Preisig, and M. Stojanovic, "Distributed space-time cooperative schemes for underwater acoustic communications," *Oceanic Engineering, IEEE Journal of*, vol. 33, no. 4, pp. 489–501, 2008.

[53] J. Han, H. Ju, K. Kim, S. Chun, and K. Dho, "A study on the cooperative diversity technique with amplify and forward for underwater wireless communication," in *OCEANS 2008-MTS/IEEE Kobe Techno-Ocean*, pp. 1–3, IEEE, 2008.

[54] Z. Han, Y. Sun, and H. Shi, "Cooperative transmission for underwater acoustic communications," in *Communications, 2008. ICC'08. IEEE International Conference on*, pp. 2028–2032, IEEE, 2008.

[55] H. Yang, F. Ren, C. Lin, and B. Liu, "Energy efficient cooperation in underwater sensor networks," in *Quality of Service (IWQoS), 2010 18th International Workshop on*, pp. 1–9, IEEE, 2010.

[56] A. Bletsas, H. Shin, M. Win, and A. Lippman, "Cooperative diversity with opportunistic relaying," in *Wireless Communications and Networking Conference, 2006. WCNC 2006. IEEE*, vol. 2, pp. 1034–1039, IEEE, 2006.

[57] Y. Jing and H. Jafarkhani, "Single and multiple relay selection schemes and their achievable diversity orders," *Wireless Communications, IEEE Transactions on*, vol. 8, no. 3, pp. 1414–1423, 2009.

[58] L. Dai, B. Gui, and L. Cimini, "Selective relaying in ofdm multihop cooperative networks," in *Wireless Communications and Networking Conference, 2007.WCNC 2007. IEEE*, pp. 963 –968, march 2007.

[59] Y. Ding and M. Uysal, "Amplify-and-forward cooperative ofdm with multiple-relays: performance analysis and relay selection methods," *Wireless Communications, IEEE Transactions on*, vol. 8, no. 10, pp. 4963–4968, 2009.

[60] J. Park, T. Do, and Y. Kim, "Outage probability of ofdm-based relay networks with relay selection," in *Vehicular Technology Conference (VTC 2010-Spring), 2010 IEEE 71st*, pp. 1–5, Ieee, 2010.

[61] B. Gui, L. Dai, and L. Cimini, "Selective relaying in cooperative ofdm systems: Two-hop random network," in *Wireless Communications and Networking Conference, 2008. WCNC 2008. IEEE*, pp. 996–1001, IEEE, 2008.

[62] J. Lee, J. Cheon, and H. Cho, "A cooperative arq scheme in underwater acoustic sensor networks," in *OCEANS 2010 IEEE-Sydney*, pp. 1–5, IEEE, 2010.

[63] S. Yerramalli and U. Mitra, "Optimal power allocation and doppler compensation in cooperative underwater networks using ofdm," in *OCEANS 2009, MTS/IEEE Biloxi-Marine Technology for Our Future: Global and Local Challenges*, pp. 1–6, IEEE, 2009.

[64] M. B. Porter, *The BELLHOP Manual and User's Guide : PRELIMINARY DRAFT*. 2011.

[65] Y. Zheng, C. Xiao, T. Yang, and W. Yang, *Frequency-domain channel estimation and equalization for single carrier underwater acoustic communications*. IEEE, 2007.

[66] J. Zhang, Y. Zheng, and C. Xiao, "Frequency-domain turbo equalization for mimo underwater acoustic communications," in *OCEANS 2009-EUROPE*, pp. 1–5, IEEE, 2009.

[67] J. Zhang and Y. Zheng, "Bandwidth-efficient frequency-domain equalization for single carrier multiple-input multiple-output underwater acoustic communications," *The Journal of the Acoustical Society of America*, vol. 128, p. 2910, 2010.

[68] K. Mackenzie, "Nine-term equation for sound speed in the oceans," *The Journal of the Acoustical Society of America*, vol. 70, p. 807, 1981.

[69] R. Urick, *Principles of underwater sound*, vol. 3. McGraw-Hill New York, 1983.

[70] M. Domingo, "Overview of channel models for underwater wireless communication networks," *Physical Communication*, vol. 1, no. 3, pp. 163–182, 2008.

[71] M. Schulkin and H. Marsh, "Sound absorption in sea water," *The Journal of the Acoustical Society of America*, vol. 34, p. 864, 1962.

[72] W. Thorp, "Analytic description of the low-frequency attenuation coefficient," *The Journal of the Acoustical Society of America*, vol. 42, p. 270, 1967.

[73] R. Mellen and D. Browning, "Low-frequency attenuation in the pacific ocean," *The Journal of the Acoustical Society of America*, vol. 59, p. 700, 1976.

[74] F. Fisher and V. Simmons, "Sound absorption in sea water," *The Journal of the Acoustical Society of America*, vol. 62, no. 3, pp. 558–564, 1977.

[75] R. Francois and G. Garrison, "Sound absorption based on ocean measurements: Part I: Pure water and magnesium sulfate contributions," *The Journal of the Acoustical Society of America*, vol. 72, p. 896, 1982.

[76] R. Francois and G. Garrison, "Sound absorption based on ocean measurements. part II: Boric acid contribution and equation for total absorption," *The Journal of the Acoustical Society of America*, vol. 72, no. 6, pp. 1879–1890, 1982.

[77] J. C. Torres, *Modelling of high-frequency acoustic propagation in shallow water*. Master Thesis, 2007.

[78] M. Stojanovic, "Underwater acoustic communications: Design considerations on the physical layer," in *Wireless on Demand Network Systems and Services, 2008. WONS 2008. Fifth Annual Conference on*, pp. 1–10, IEEE, 2008.

[79] P. Qarabaqi and M. Stojanovic, "Modeling the large scale transmission loss in underwater acoustic channels," in *Communication, Control, and Computing (Allerton), 2011 49th Annual Allerton Conference on*, pp. 445–452, IEEE, 2011.

[80] B. Li, S. Zhou, M. Stojanovic, L. Freitag, and P. Willett, "Multicarrier communication over underwater acoustic channels with nonuniform doppler shifts," *Oceanic Engineering, IEEE Journal of*, vol. 33, no. 2, pp. 198–209, 2008.

[81] R. Coates, *Underwater acoustic systems*. Halsted Press, 1989.

[82] M. Porter and H. Bucker, "Gaussian beam tracing for computing ocean acoustic fields," *The Journal of the Acoustical Society of America*, vol. 82, p. 1349, 1987.

[83] P. Etter, *Underwater acoustic modeling and simulation*. Taylor & Francis, 2003.

[84] K. Koprulu, *Acoustic propagation model applications in the Mediterranean and Black Sea regions*. Master Thesis, 2006.

[85] "National geophysical data center." `http://www.ngdc.noaa.gov/mgg/global/global.html`.

[86] "General bathymetric chart of the oceans." `http://http://www.gebco.net`.

[87] "National geophysical data center, seafloor surficial sediment descriptions.." `http://www.ngdc.noaa.gov/mgg/geology/deck_41.html`.

[88] M. Olfat, F. Farrokhi, and K. Liu, "Power allocation for ofdm using adaptive beamforming over wireless networks," *Communications, IEEE Transactions on*, vol. 53, no. 3, pp. 505–514, 2005.

[89] K. Al-Mawali, A. Sadik, and Z. Hussain, "Low complexity discrete bit-loading for ofdm systems with application in power line communications," *Int'l J. of Communications, Network and System Sciences*, vol. 4, no. 6, pp. 372–376, 2011.

[90] A. Goldsmith, *Wireless communications*. Cambridge Univ Press, 2005.

[91] S. Talwar, Y. Jing, and S. Shahbazpanahi, "Joint relay selection and power allocation for two-way relay networks," *Signal Processing Letters, IEEE*, vol. 18, no. 2, pp. 91–94, 2011.

[92] L. Song, "Relay selection for two-way relaying with amplify-and-forward protocols," *Vehicular Technology, IEEE Transactions on*, no. 99, pp. 1–1, 2011.

[93] M. Dong and S. Shahbazpanahi, "Optimal spectrum sharing and power allocation for ofdm-based two-way relaying," in *Acoustics Speech and Signal Processing (ICASSP), 2010 IEEE International Conference on*, pp. 3310–3313, IEEE, 2010.

[94] F. Pancaldi, G. Vitetta, R. Kalbasi, N. Al-Dhahir, M. Uysal, and H. Mheidat, "Single-carrier frequency domain equalization," *Signal Processing Magazine, IEEE*, vol. 25, no. 5, pp. 37–56, 2008.

[95] H. Mheidat, M. Uysal, and N. Al-Dhahir, "Equalization techniques for distributed space-time block codes with amplify-and-forward relaying," *Signal Processing, IEEE Transactions on*, vol. 55, no. 5, pp. 1839–1852, 2007.

[96] Z. Wang, X. Ma, and G. Giannakis, "Ofdm or single-carrier block transmissions?," *Communications, IEEE Transactions on*, vol. 52, no. 3, pp. 380–394, 2004.

[97] A. Tajer and A. Nosratinia, "Diversity order in ISI channels with single-carrier frequency-domain equalizers," *Wireless Communications, IEEE Transactions on*, vol. 9, no. 3, pp. 1022–1032, 2010.

VITA

Hamza Ümit Sökün was born in Istanbul on the first of March, 1986. He received a Bachelor of Science in electronic engineering (with a double major in computer engineering) with high honors, from Kadir Has University in Istanbul, May of 2010. Then, he began work toward a Master of Science in Electrical and Electronic Engineering at Özyeğin University in the Fall of 2010.